
InSAR DEFORMATION MONITORING General's Highway, Sequoia National Park

Publication No. FHWA-CFL/TD-09-003

July 2009



U.S. Department
of Transportation
**Federal Highway
Administration**

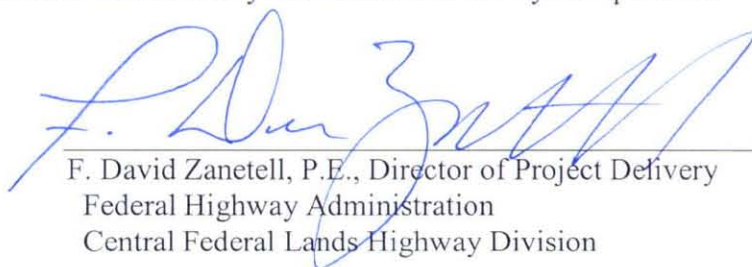


**Central Federal Lands Highway Division
12300 West Dakota Avenue
Lakewood, CO 80228**

FOREWORD

The Federal Lands Highway (FLH) of the Federal Highway Administration (FHWA) promotes development and deployment of applied research and technology applicable to solving transportation related issues on Federal Lands. The FLH provides technology delivery, innovative solutions, recommended best practices, and related information and knowledge sharing to Federal agencies, Tribal governments, and other offices within the FHWA.

The use of Interferometric Synthetic Aperture Radar (InSAR) to measure ground movement, especially where landslides intersect with roadway corridors are of interest to the FLH. Knowing the rate of vertical, lateral extent, and direction of the movement all are key pieces of information for geotechnical engineers and roadway designers. The results of this InSAR study demonstrate the level of accuracy for which landslide movement may be obtained for use by transportation engineers.



F. David Zanetell, P.E., Director of Project Delivery
Federal Highway Administration
Central Federal Lands Highway Division

Notice

This document is disseminated under the sponsorship of the U.S. Department of Transportation in the interest of information exchange. The U.S. Government assumes no liability for the use of the information contained in this document. This report does not constitute a standard, specification, or regulation.

The U.S. Government does not endorse products or manufacturers. Trademarks or manufacturers' names appear in this report only because they are considered essential to the objective of the document.

Quality Assurance Statement

The FHWA provides high-quality information to serve Government, industry, and the public in a manner that promotes public understanding. Standards and policies are used to ensure and maximize the quality, objectivity, utility, and integrity of its information. FHWA periodically reviews quality issues and adjusts its programs and processes to ensure continuous quality improvement.

Technical Report Documentation Page

1. Report No. FHWA-CFL/TD-09-003	2. Government Accession No.	3. Recipient's Catalog No.	
4. Title and Subtitle <i>InSAR Deformation Monitoring General's Highway, Sequoia National Park</i>		5. Report Date July 2009	
		6. Performing Organization Code	
7. Author(s) Shinya Sato, Bert Kampes, Marco van der Kooij, Allan Place		8. Performing Organization Report No. 2006-4-0143	
9. Performing Organization Name and Address MDA Geospatial Services Inc. Unit 110 - 20 Colonnade Road Ottawa, Ontario, Canada K2E 7M6		10. Work Unit No. (TRAIS)	
		11. Contract or Grant No. DTFH68-06-P-00195	
12. Sponsoring Agency Name and Address Federal Highway Administration Central Federal Lands Highway Division 12300 W. Dakota Avenue, Suite 210 Lakewood, CO 80228		13. Type of Report and Period Covered Final Report September 2006 – February 2008	
		14. Sponsoring Agency Code HFTS-16.4	
15. Supplementary Notes COTR: Roger Surdahl, FHWA-CFLHD; Advisory Panel Members: Scott Anderson, FHWA-RC; Khamis Haramy, Alan Blair, Pat Flynn, and Beau Williams, FHWA-CFLHD. This project was funded under the Federal Lands Highway Technology Deployment Initiatives and Partnership Program (TDIPP).			
16. Abstract Ground movement was monitored using Interferometric Synthetic Aperture Radar (InSAR) coupled with on-site corner reflector technology for an area where the General's Highway in the Sequoia National Park, California crossed over an unstable slope. As part of proposed roadway improvements for this section, one corner reflector was placed on a known stable rock outcrop, and two corner reflectors were placed in known unstable locations on the slope above and below the roadway. This study found some minimal InSAR deformation at the corner reflector locations over a four month period of 1.7 to 2.5 mm vertical movement, and 2.3 to 3.4 mm on the flow line.			
17. Key Words InSAR, SLOPE STABILITY, GROUND MOVEMENT, CORNER REFLECTORS		18. Distribution Statement No restriction. This document is available to the public from the sponsoring agency at the website http://www.cflhd.gov .	
19. Security Classif. (of this report) Unclassified	20. Security Classif. (of this page) Unclassified	21. No. of Pages 48	22. Price

InSAR DEFORMATION MONITORING – TABLE OF CONTENTS

SI* (MODERN METRIC) CONVERSION FACTORS				
APPROXIMATE CONVERSIONS TO SI UNITS				
Symbol	When You Know	Multiply By	To Find	Symbol
LENGTH				
in	Inches	25.4	Millimeters	mm
ft	feet	0.305	Meters	m
yd	yards	0.914	Meters	m
mi	miles	1.61	Kilometers	km
AREA				
in ²	Square inches	645.2	Square millimeters	mm ²
ft ²	Square feet	0.093	Square meters	m ²
yd ²	Square yard	0.836	Square meters	m ²
ac	acres	0.405	Hectares	ha
mi ²	Square miles	2.59	Square kilometers	km ²
VOLUME				
fl oz	fluid ounces	29.57	Milliliters	mL
gal	gallons	3.785	Liters	L
ft ³	cubic feet	0.028	cubic meters	m ³
yd ³	cubic yards	0.765	cubic meters	m ³
NOTE: volumes greater than 1000 L shall be shown in m ³				
MASS				
oz	ounces	28.35	Grams	g
lb	pounds	0.454	Kilograms	kg
T	short tons (2000 lb)	0.907	megagrams (or "metric ton")	Mg (or "t")
TEMPERATURE (exact degrees)				
°F	Fahrenheit	5 (F-32)/9 or (F-32)/1.8	Celsius	°C
ILLUMINATION				
fc	foot-candles	10.76	Lux	lx
fl	foot-Lamberts	3.426	candela/m ²	cd/m ²
FORCE and PRESSURE or STRESS				
lbf	Poundforce	4.45	Newtons	N
lbf/in ²	Poundforce per square inch	6.89	Kilopascals	kPa
APPROXIMATE CONVERSIONS FROM SI UNITS				
Symbol	When You Know	Multiply By	To Find	Symbol
LENGTH				
mm	millimeters	0.039	Inches	in
m	Meters	3.28	Feet	ft
m	Meters	1.09	Yards	yd
km	kilometers	0.621	Miles	mi
AREA				
mm ²	Square millimeters	0.0016	square inches	in ²
m ²	Square meters	10.764	square feet	ft ²
m ²	Square meters	1.195	square yards	yd ²
ha	hectares	2.47	Acres	ac
km ²	Square kilometers	0.386	square miles	mi ²
VOLUME				
mL	milliliters	0.034	fluid ounces	fl oz
L	liters	0.264	Gallons	gal
m ³	cubic meters	35.314	cubic feet	ft ³
m ³	cubic meters	1.307	cubic yards	yd ³
MASS				
g	Grams	0.035	Ounces	oz
kg	kilograms	2.202	Pounds	lb
Mg (or "t")	megagrams (or "metric ton")	1.103	short tons (2000 lb)	T
TEMPERATURE (exact degrees)				
°C	Celsius	1.8C+32	Fahrenheit	°F
ILLUMINATION				
lx	Lux	0.0929	foot-candles	fc
cd/m ²	candela/m ²	0.2919	foot-Lamberts	fl
FORCE and PRESSURE or STRESS				
N	newtons	0.225	Poundforce	lbf
kPa	Kilopascals	0.145	poundforce per square inch	lbf/in ²

*SI is the symbol for the International System of Units. Appropriate rounding should be made to comply with Section 4 of ASTM E380. (Revised March 2003)

ABBREVIATIONS, ACRONYMS AND SYMBOLS

Abbreviations

CR	Corner Reflector
CTM	Coherent Target Monitoring
DEM	Digital Elevation Model
EOServ	Earth Observation Services department (Vexcel)
InSAR	Interferometric Synthetic Aperture Radar
FHWA	Federal Highway Administration
FLH	Federal Lands Highway
GPS	Global Positioning Satellite
LOS	Line-Of-Sight between sensor and observed pixel in the terrain
MDA	MacDonald Dettwiler and Associates Inc.
RADAR	Radio Detection and Ranging
SAR	Synthetic Aperture Radar
SCR	Signal-to-Noise Ratio
USGS	United States Geological Survey

Symbols

B _{perp}	Perpendicular baseline: distance between sensors in space.
dT	Temporal baseline: the time between two acquisitions.
σ_{phase}	standard deviation of phase
σ_{LOS}	standard deviation of line-of-sight measurement in millimeters
λ	Wavelength
θ	incidence angle

TABLE OF CONTENTS

CHAPTER 1 – EXECUTIVE SUMMARY	1
CHAPTER 2 – INTRODUCTION	3
InSAR PROCESSING OVERVIEW	3
CHAPTER 3 – PROJECT OVERVIEW	7
PROJECT OBJECTIVE AND SCOPE	7
STUDY AREA	7
SATELLITE DATA	9
REFLECTOR HEIGHT UNCERTAINTY	9
CHAPTER 4 – CORNER REFLECTOR ANALYSIS	11
CORNER REFLECTOR INSTALLATION	11
CORNER REFLECTOR DETECTION	11
CHOICE OF THE REFERENCE POINT	13
SLANT RANGE CHANGE DEFORMATION PROFILE	14
FLOW-LINE DEFORMATION	20
CHAPTER 5 – CONVENTIONAL INSAR DEFORMATION MAPS	25
RESULTS	25
CHAPTER 6 – CONCLUSIONS	31
APPENDIX A – EXAMPLE DELIVERABLES	33
APPENDIX B – NOTES ON CORNER REFLECTOR INSTALLATION	35

LIST OF FIGURES

Figure 1. Drawing. Radar imaging principle.3

Figure 2. Schematic. Interferometric phase measurements at two locations.....4

Figure 3. Map. Sequoia National Park Slide Area.....8

Figure 4. Photos. Installed Corner Reflectors.....11

Figure 5. Map. Average Amplitude Image.12

Figure 6. Chart. Slant range change profiles for the installed Corner Reflector #1.15

Figure 7. Chart. Slant range change profiles for the installed Corner Reflector #2.16

Figure 8. Chart. Slant range change profiles for the installed Corner Reflector #3.17

**Figure 9. Map. Cumulative slant-range-change from September 25, 2007 to
October 19, 2007.....18**

**Figure 10. Map. Cumulative slant-range-change from September 25, 2007 to
December 6, 2007.19**

**Figure 11. Map. Cumulative slant-range-change from September 25, 2007 to
December 30, 2007.20**

Figure 12. Schematic. Geometry for flow-line deformation computation.....22

**Figure 13. Schematic. Slant range change map for the time period August 8, 2007 to
October 19, 2007 (Pair A).....26**

**Figure 14. Schematic. Slant range change map for the time period December 6, 2007 to
December 30, 2007 (Pair B).....27**

LIST OF TABLES

Table 1. Location of Corner Reflectors.....7

Table 2. Scheduled and used data for this project.....9

Table 3. Baselines and height ambiguity for the InSAR pairs used to measure the CRs.9

Table 4. Estimated Signal-to-Clutter ratios for each Corner Reflector in each acquisition.13

Table 5. Visibility of the Corner Reflectors.....13

Table 6. Cumulative slant range deformation in millimeters at the Corner Reflectors.....14

Table 7. Parameters used for flow-line deformation computation.....21

Table 8. Flow-line deformation measurements.23

Table 9. Deformation measurements from Pair A.....28

Table 10. Deformation measurements from Pair B.....28

Table 11. Estimated noise level of Pair A.28

Table 12. Estimated noise level of Pair B.....29

Table 13. Estimated noise level summary of Pair A.29

Table 14. Estimated noise level summary of Pair B.29

Table 15. Delivered digital files.....33

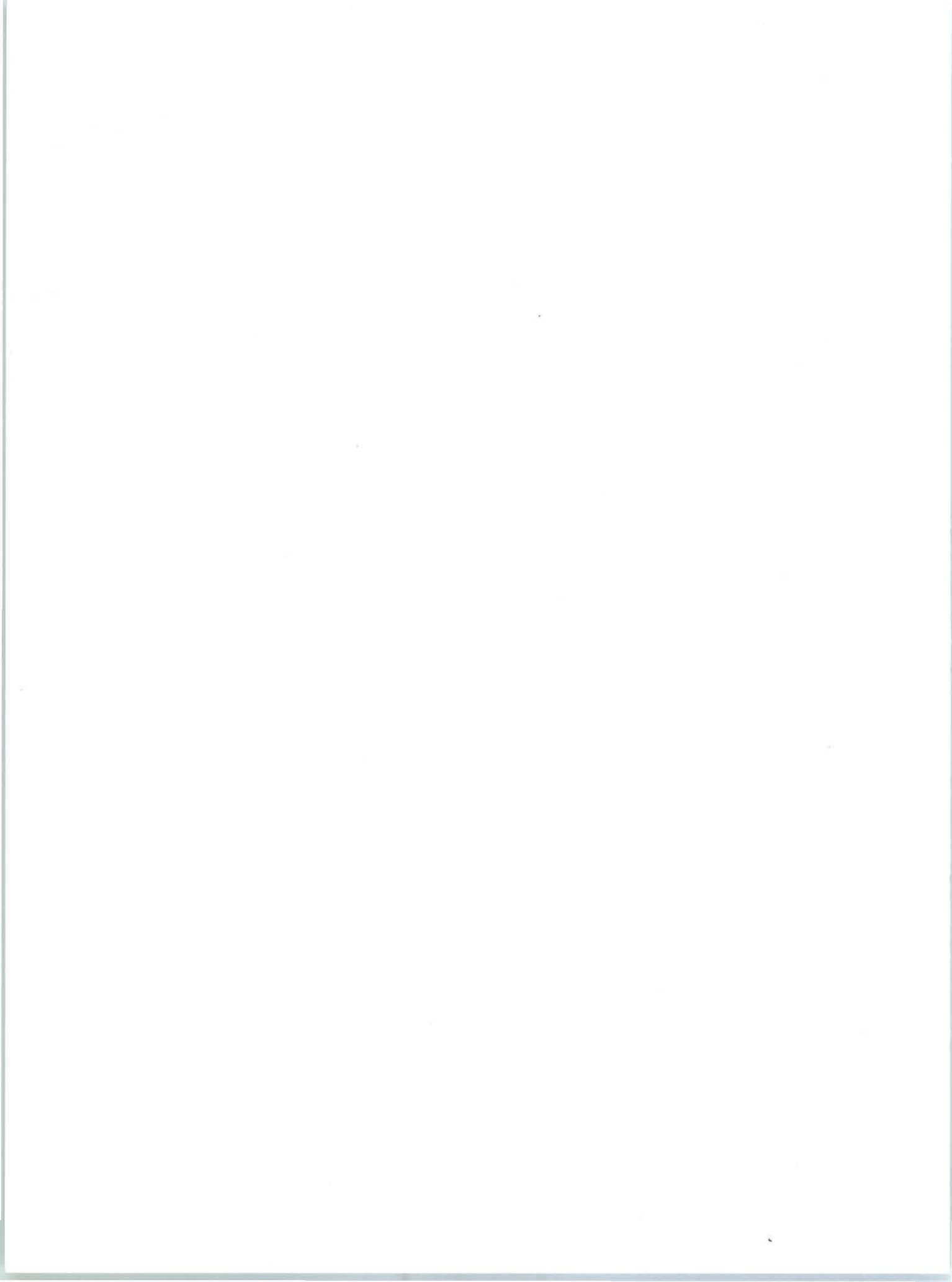
CHAPTER 1 – EXECUTIVE SUMMARY

This final report describes the Interferometric Synthetic Aperture Radar (InSAR) processing that was performed to monitor deformation of a slow-moving landslide at General's Highway in Sequoia National Park, California, in 2007. This report focuses on the deformation measurements made on three Corner Reflectors (CRs) that were deployed at that location by Federal Highway Administration, Federal Lands Highway with the permission of the Sequoia National Park. Additionally two conventional deformation maps were produced.

The three CRs were successfully installed on September 18 and 19, 2007 by FHWA personal. These CRs were scheduled for observation by satellite and four acquired RADARSAT-1 satellite images were used to measure deformation at these three locations, from September 25, 2007 to December 30, 2007. The CRs were successfully detected from the four acquired RADARSAT images. The observed down-hill deformation had a maximum of 2.5 mm for CR#2 (Upper Slide Reflector) and 1.7 mm at CR#3 (Lower Slide Reflector), relative to the reference CR#1 (Stable Reflector), which was assumed to be not moving. The precision of the deformation measurements is computed as approximately 0.9 mm. The detected movement was consistent in direction and rate in the observed time period.

Ten radar images were processed to create deformation maps with InSAR for this project. A conventional interferometric deformation map can be generated if the spatial coherence for an interferometric data pair is above a certain threshold. This map shows the deformation patterns outside of the CRs locations, but cannot always be generated (hence the usage of the CRs). For this study, the observed slope can be well seen by the satellites geometrically, however the noise due to temporal de-correlation is significant. No large deformation phenomena were observed in the two deformation maps.

The precise deformation observations using CRs at this site clearly demonstrate the potential for usage of CRs. It was unfortunate that the installation of the CR was delayed until mid September, and only four measurements could be made. Moreover, the exact 3D position of the CRs was not measured during installation, which limited the accuracy during processing. While their latitude and longitude were recorded for each corner reflector, the vertical elevation was not. The quality of the measurements increases with better knowledge of the height of the CRs. However, the baselines of the data pairs used were limited, and therefore the sensitivity to height errors, and we are confident the heights as used in this report (based on a precise Digital Elevation Model) are close to the actual heights. For future monitoring of any CRs, it is recommended that the precise 3D position be measured.



CHAPTER 2 – INTRODUCTION

MDA Geospatial Services Inc. has executed hundreds of projects using InSAR technology since 1997. The main objective of these projects was to create very accurate surface deformation maps using space borne radar technology.

This report describes the deformation monitoring at General's Highway in Sequoia National Park during 2007. The report gives a brief introduction in InSAR deformation mapping technology and provides details on the actual processing.

InSAR PROCESSING OVERVIEW

Synthetic Aperture Radar (SAR) systems measure both the magnitude and the phase of microwave energy backscatter from the earth's surface of a transmitted electromagnetic signal, produced by a radar camera on board a satellite. The magnitude is usually associated with a remotely sensed image as shown in Figure 1. It indicates the "brightness" of the surface as detected by the SAR. The phase represents the combination of two factors: (i) the distance from the SAR to the surface, and (ii) the surface scattering effect on the incident electromagnetic wave as shown in Figure 2. Given that this scattering effect is independent from point-to-point on the ground, the phase of a single SAR image is in general random, and of no practical purpose on its own.

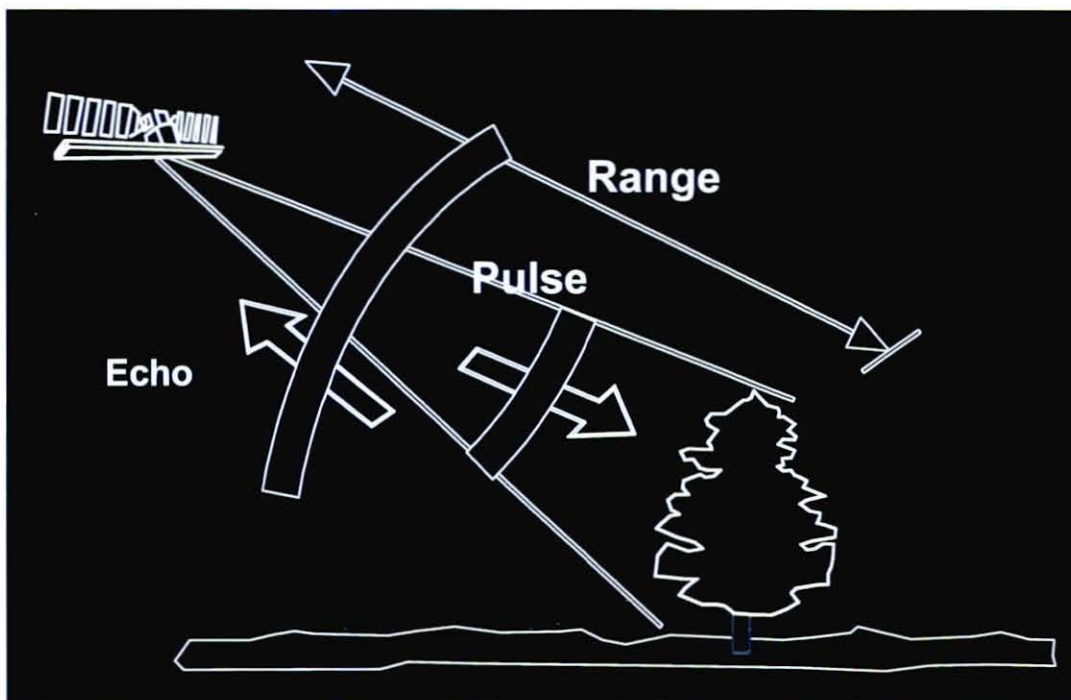


Figure 1. Drawing. Radar imaging principle.

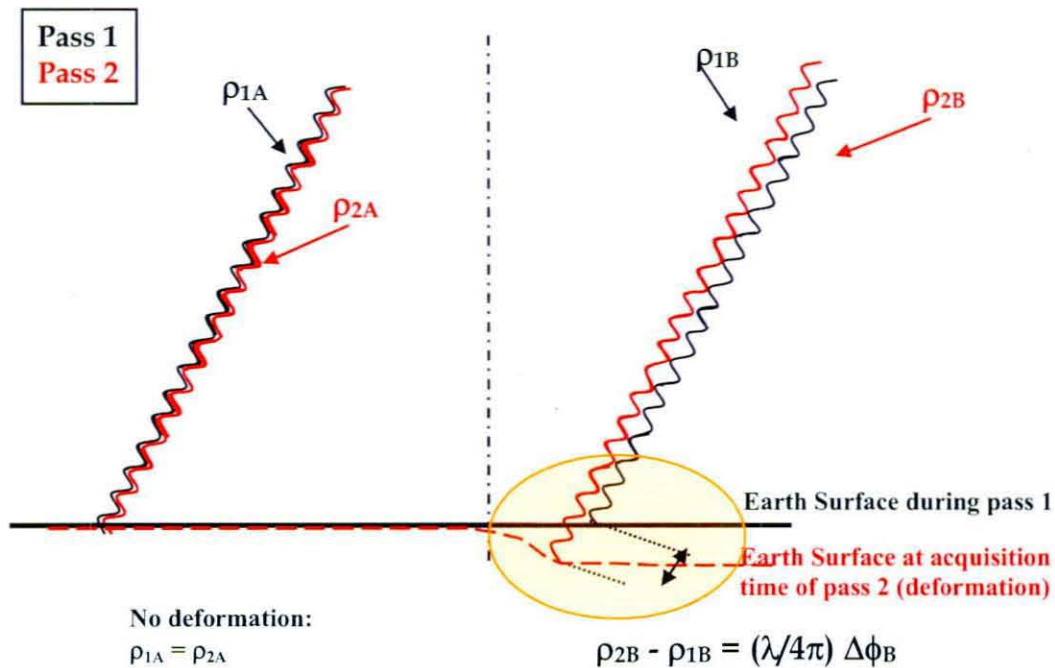


Figure 2. Schematic. Interferometric phase measurements at two locations. The left panel represents a pixel (A) in the interferogram where the surface did not undergo deformation in the time between the acquisitions of pass 1 (black) and pass 2 (red), resulting in a zero interferometric phase. The distances ρ_{1A} and ρ_{2A} are equal. The right panel shows a pixel (B) where the terrain has subsided: the interferometric phase difference $\Delta\phi_B$ that can be measured is related to the change in distance of the terrain to the sensor $\rho_{2B} - \rho_{1B}$, between pass 1 and pass 2, and to the wavelength λ .

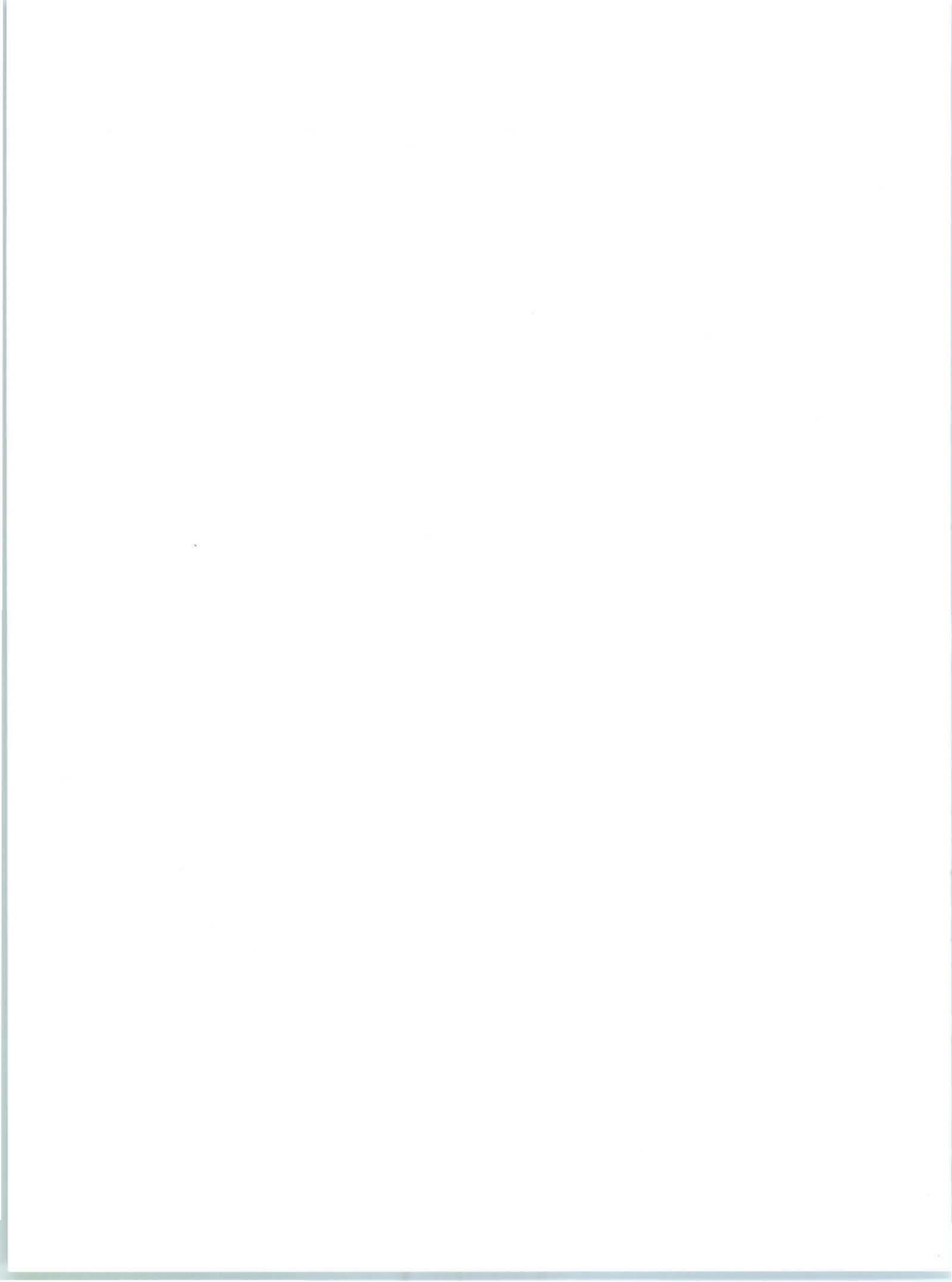
If a second SAR data set is collected from nearly the same location in space as the first image, then upon subtraction of the phase of the second image from the first, an interferogram is formed, see also Figure. Hence the term Interferometric SAR (InSAR). If the distance, called the baseline, between the two locations of the SAR platform in space is small then the surface scattering effects will be the same for the two images and are thus canceled in the formation of the interferogram. Therefore the interferogram exhibits information related to the difference in distances from the surface to the two SAR locations. Knowing the geometry involved, topographic heights can be computed from this information. It has been shown that the sensitivity of the phase to height is proportional to the baseline, i.e., there will be more interferometric phase induced by topography if the baseline is larger. The precisions of terrain height measurements are typically 1 to 10 meters, depending on the value of the baseline and noise.

If surface deformation occurred between the acquisition times of the two imaging passes of the SAR platform, then the interferogram phase represents a combination of topographic information and surface change. If the topography for the area is known with a sufficient precision, it can be used to remove the topographic phase information from the interferogram, leaving only the surface change phase. The sensitivity of the phase to surface change is in the order of a fraction

($\sim 1/100$) of the wavelength of the transmitted electromagnetic wave, which is ~ 5.6 centimeter for the C-Band SAR used in this project. Thus, the precision of the surface change measurement is at the millimeter level.

The processing steps to generate a deformation map using InSAR are:

1. Historic SAR data set selection or future acquisition scheduling.
2. Raw SAR data processing: Two SAR scenes are processed to a product that includes magnitude information and phase information.
3. Image coregistration: Both scenes are very accurately co-registered (lined up) to sub-pixel accuracy.
4. Interferogram generation: The interferogram is an image of the phase difference between corresponding pixels of the 2 images.
5. Topographic phase removal: An external Digital Elevation Model (DEM) is used to remove effects of stationary topography.
6. Phase unwrapping: For the generation of a quantitative deformation product it is crucial to create a map of “absolute phase” from “wrapped phase” values. This process is called “phase unwrapping”.
7. Terrain distortion correction (ortho-rectification): This process removes specific image distortions due to the radar geometry.
8. Ground control point collection and position refinement: This process is required as the inherent geo-referencing of the SAR data is not accurate enough. Ground control points from standard topographical maps are generally sufficient to achieve horizontal position accuracies of ~ 20 m.
9. Deformation map generation in specific format and projection/datum.



CHAPTER 3 – PROJECT OVERVIEW

This section briefly describes the location and setting of the project area, as well as the available data.

PROJECT OBJECTIVE AND SCOPE

The objective of this project was to provide the FHWA with measurements of the deformation that occurred at the project's area of interest using InSAR monitoring. Two strategies were followed: (i) Three CRs were deployed, analyzed, and measured, which provided precise deformation measurements at these locations; (ii) conventional InSAR deformation maps were produced when possible, which depended on the level of temporal de-correlation in the data.

The contract deliverables included deformation maps quantifying movement that occurred in 2007. For this study deformation maps and deformation profiles were produced for four measurement times focused on the three CRs. Appendix A shows the type of deliverables typically provided on studies like this.

STUDY AREA

At the time the CRs were installed, their latitude and longitude were recorded using a hand-held GPS unit, as noted in Appendix B and shown in Table 1. Unfortunately, their vertical component of elevation was not reported.

Table 1. Location of Corner Reflectors.

Corner Reflector	Latitude	Longitude	Height (m)
Measurements that used for this Study			
CR#1 (Stable Reflector)	N36° 32.572'	W118° 47.035'	1480.26
CR#2 (Upper Slide Reflector)	N36° 32.568'	W118° 47.098'	1503.59
CR#3 (Lower Slide Reflector)	N36° 32.558'	W118° 47.065'	1467.35
Measurements taken for comparison at the removal of the Corner Reflectors, but that were not used for this Study			
CR#1 (Stable Reflector)	N36° 32.5742'	W118° 47.0338'	1491.6
CR#2 (Upper Slide Reflector)	N36° 32.5787'	W118° 47.1028'	1497.5
CR#3 (Lower Slide Reflector)	N36° 32.5602'	W118° 47.0646'	1484.6

Subsequently, their heights were obtained from the USGS 10 m DEM data, interpolated at the given coordinates. Also as noted in Appendix B, the reported latitude for the CR#1 was corrected. The CRs positions used in this study are shown in Table 1. As a check to these values, when the FHWA removed the CRs on August 6, 2008, their positions were again recorded using another hand-held GPS unit. While these follow-up measurements are shown in Table 1, they were not used in this study, and are provided only as comparative information. This illustrates the need to accurately measure CRs locations with reliable tools. Figure 3 shows an overview of the project area.

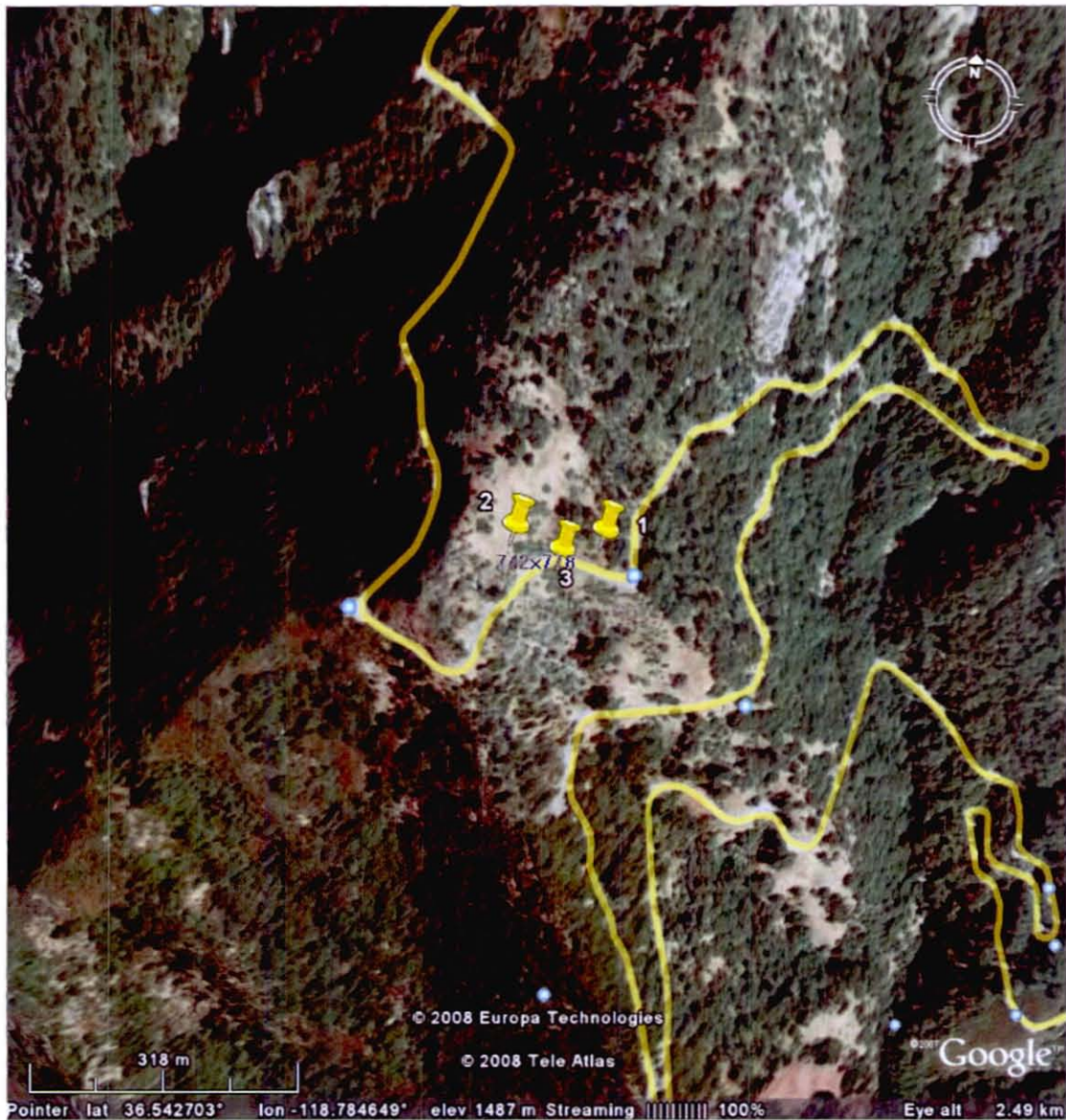


Figure 3. Map. Sequoia National Park Slide Area. Corner Reflector locations are noted by the yellow pushpins.

SATELLITE DATA

Table 2 shows an overview of the data that were collected and used in this study. In total, 18 images were scheduled for acquisition for this project, and 10 images were processed.

Table 2. Scheduled and used data for this project. Highlighted data images that were processed (green for S1; orange for F2; blue F2 after Corner Reflector installation).

Scheduled #	Used #	Acquisition Date	Look Direction	Orbit Number	Beam Mode	Perpendicular Baseline
1	1	1-Jan-07	Asc	58246	S1	0
2		25-Jan-07	Asc	58589	S1	-935
3	2	18-Feb-07	Asc	58932	S1	223
4		14-Mar-07	Asc	59275	S1	-574
5		4-Apr-07	Asc	59618	S1	-823
6	3	1-May-07	Asc	59961	S1	160
7		25-May-07	Asc	60304	S1	-1060
8	4	18-Jun-07	Asc	60647	S1	278
9		12-Jul-07	Asc	60990	S1	-892
10	5	21-Jun-07	Asc	60690	F2	0
11		15-Jul-07	Asc	61033	F2	-1547
12	6	8-Aug-07	Asc	61376	F2	-223
13		1-Sep-07	Asc	61719	F2	-915
14	7	25-Sep-07	Asc	62062	F2	-268
15	8	19-Oct-07	Asc	62405	F2	-312
16		12-Nov-07	Asc	62748	F2	-832
17	9	6-Dec-07	Asc	63091	F2	-518
18	10	30-Dec-07	Asc	63434	F2	-515

REFLECTOR HEIGHT UNCERTAINTY

The height of the CRs was not measured at installation, and therefore was obtained from the USGS 10 m DEM for this project. This introduced uncertainty in the measured deformation profiles. Table 3 lists the baselines and height ambiguity for the interferograms used to compute the deformation at the CRs locations.

Table 3. Baselines and height ambiguity for the InSAR pairs used to measure the Corner Reflectors. The master and slave numbers correspond to Column 2 of Table 2. A smaller baseline implies less sensitivity to height and a larger height ambiguity. This was preferred for deformation mapping.

Interferogram	Master-Slave	Baseline (m)	Height Ambiguity (m/cycle)
1	7-8	44	-285
2	8-9	206	-85
3	9-10	3	-3590

The height ambiguity is the topographic difference between points that would induce one phase cycle in the interferogram. Interferograms with a small baseline are less sensitive to topography. For example, interferogram #3 with a baseline of 3 meter is hardly sensitive to topographic height. If a mountain of 3590 meters high would be present in the image, it would only induce 1 phase cycle. On the other hand, for interferogram #2, the baseline is 206 m and the height ambiguity is 85 m. The same 3590 meter mountain would show up in this interferogram as $3590/85 = 42.24$ phase cycles.

For the application of deformation monitoring, the known topography is removed from the interferograms. It is important to realize that the topographic height is never known exactly, which implies that residual topographic signal remains in the interferogram as phase. This will in turn be interpreted incorrectly as deformation signal. To assess the magnitude of this error, assume that the mountain actually was 3600 m, while the DEM used said it was 3590 meters. For interferogram 3, this 10 meter error will result in $10/3590=0.002$ phase cycles. One cycle corresponds to 28 mm of deformation, so this can be ignored. For the interferogram #2, the 10 meter topographic error leads to $10/85=0.12$ phase cycles, or about 3.3 mm of incorrectly estimated deformation. For interferogram #1 the height ambiguity is about 3 times more than interferogram #2, which means that the error in deformation will be a factor 3 less.

The heights of the CRs obtained by interpolation of the USGS 10 meter DEM were expected to be precise to a few meters. This means that the delivered deformation profiles have an error of at most 1 to 2 mm caused by this inaccuracy compared to their actual heights. Ideally, and for future monitoring of these CRs, the actual heights should be obtained by GPS. Note that only the relative heights of the CR#2 and CR#3 to CR#1 need to be known precisely; an error in the absolute height of the CRs does not propagate to an error in the deformation profiles, but errors of the height differences do.

Note that the baselines used for this project were rather small, which was somewhat fortunate and it was also the reason that these interferograms were selected from all acquired data. Moreover, the baselines were random in magnitude and sign, which implied that the errors in the deformation profiles were expected to average out over time.

CHAPTER 4 – CORNER REFLECTOR ANALYSIS

The reflected signal from deployed CRs can be detected by the radar, and precise measurements can be made using the phase of the complex radar signal. These measurements are transformed to slant range change and flow-line deformation measurements.

CORNER REFLECTOR INSTALLATION

The three CRs were installed on September 17 and 18, 2007, by members of the Federal Highway Administration, Federal Lands Highway team who sponsored this study. The CRs were carefully fixed to their pilings, and were aligned to the satellite. Figure 4 shows the three CRs.

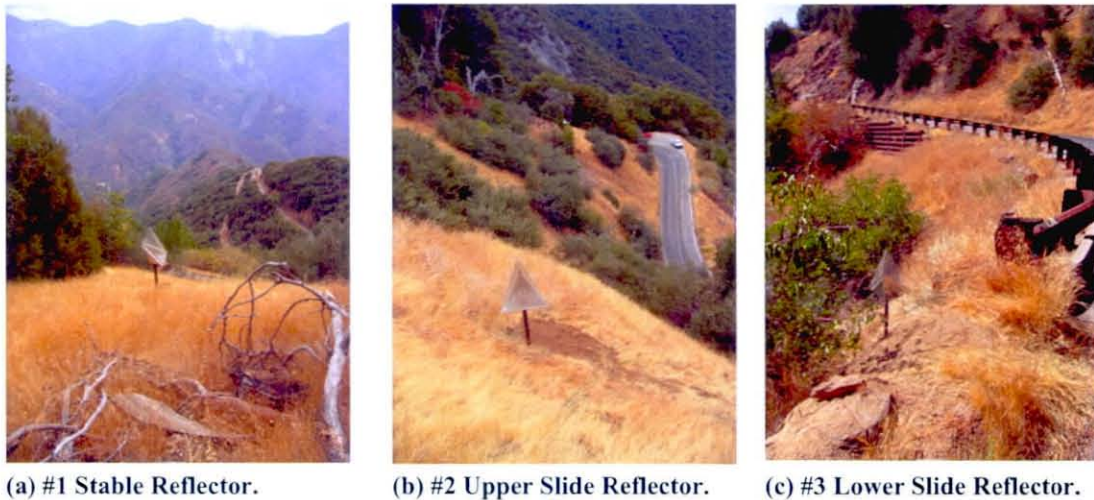


Figure 4. Photos. Installed Corner Reflectors.

While the CRs were planned to be fully part of this study, their installation was delayed due to international customs import issues and shipping complications. Because of the delayed CRs installation date, measurements could only be made for the last part of the year. However, the CRs were installed in difficult terrain and orientated in the correct direction in good communication between MDA and FHWA. Only the latitude and longitude positions were recorded and this complicated the processing as precise knowledge of the height (differences) between CRs was essential for InSAR processing. For this study, the heights were obtained at the provided locations using the USGS 10m DEM.

CORNER REFLECTOR DETECTION

The first step in the analysis of the CRs was the detection in the imagery. The three CRs could be identified relatively easy in the four SAR data acquired after September 18, 2007. Figure 5

shows the average of the radar images acquired after September 18, 2007. The location of the CRs can be easily seen as high backscatter dots in this image.

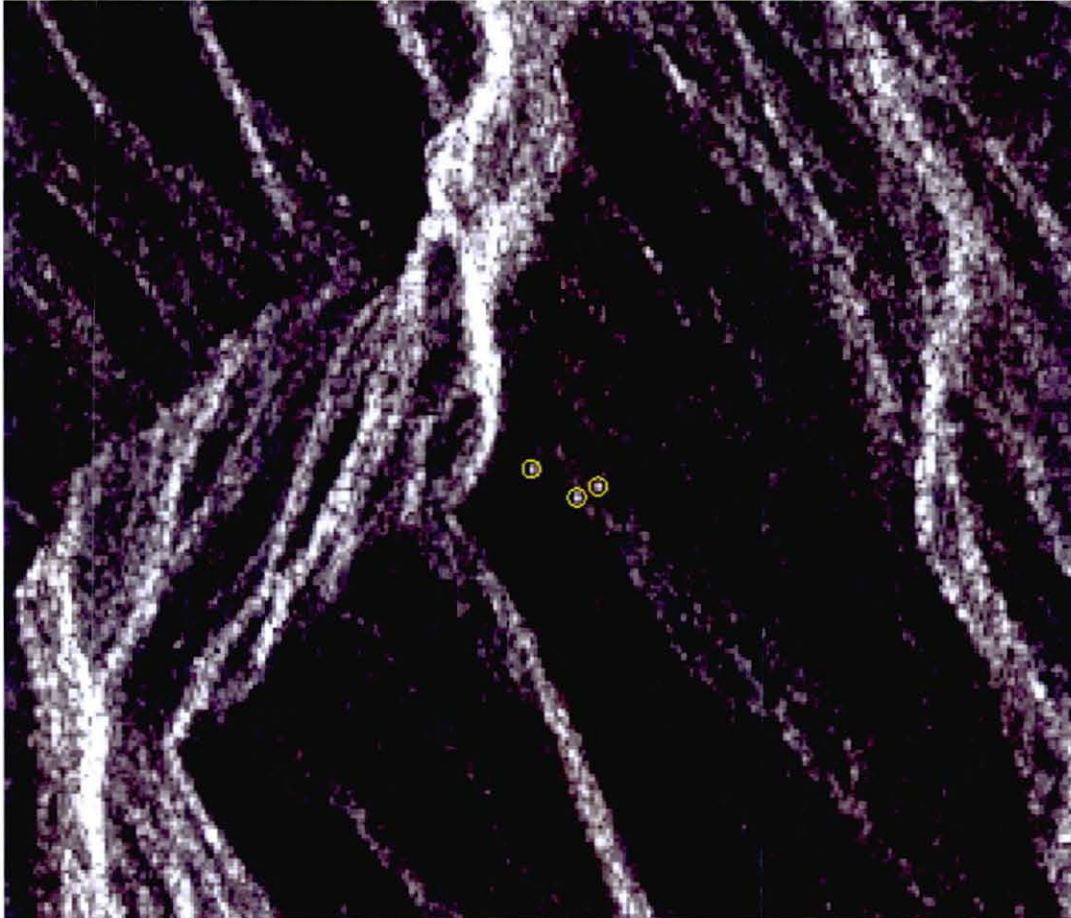


Figure 5. Map. Average Amplitude Image. The Corner Reflectors are clearly visible as bright dots inside of the yellow circles. This indicates a strong reflection back to the radar. This image is in the radar geometry and only coarsely geo-referenced to avoid aliasing and interpolation effects.

The brightness of the return can be related to the precision of the slant range change measurements as follows. The Signal-to-Clutter Ratio (SCR) is related to the phase standard deviation, and therefore to the precision of the deformation measurements, approximately as

$$\sigma_{phase} = \frac{1}{\sqrt{2 \cdot SCR}} \text{ [rad]},$$

$$\sigma_{LOS} = \frac{\lambda}{4\pi} \cdot \sigma_{phase} \approx 4.5 \cdot \sigma_{phase} \text{ [mm]}$$

using the wavelength of the carrier frequency used by RADARSAT ($\lambda=5.66$ centimeter) and the approximate local incidence angle of $\theta=40$ degrees.

Table 4 lists the estimated SCR values. These values were related to the expected precisions of the measurements, based on evaluation of real data measurements (amplitude). For example, an SCR of 80 maps to a standard deviation of the slant range change of 0.36 mm; an SCR of 40 to a standard deviation of 0.50 mm; and an SCR of 10 to 1.01 mm.

Table 4. Estimated Signal-to-Clutter ratios for each Corner Reflector in each acquisition. The average SCR was 52.0, corresponding to a standard deviation (measurement precision) of 0.44 mm of the measured slant range change at a single point in a single image.

CRs	Sep 25, 2007	Oct 19, 2007	Dec 6, 2007	Dec 30, 2007	Average	Precision
CR#1	48.8	92.5	18.7	26.4	46.6	0.46 mm
CR#2	27.6	153.3	54.8	34.6	67.6	0.39 mm
CR#3	36.2	44.2	25.6	61.2	41.8	0.49 mm
Average	37.5	96.7	33.0	40.7	52.0	0.44 mm

It should be noted that the deformation measurements were derived from the single image, single point phase measurements by taking two differences in space and in time. Therefore, the expected standard deviation of the delivered measurements was a factor two larger than the single point single image standard deviation that is, on average approximately 0.88 mm, based on this analysis.

All three CRs were identified as shown in Table 5 in the all imagery acquired after September 18, 2007, which was their installation date. The estimated standard deviation of the delivered slant range change measurements was 0.88 mm, based on the average Signal-to-Clutter Ratio of the detected CRs.

Table 5. Visibility of the Corner Reflectors. Items marked with X were not reliable and not delivered. The installed Corner Reflectors performed excellently.

CRs	Sep 25, 2007	Oct 19, 2007	Dec 6, 2007	Dec 30, 2007
CR#1	✓	✓	✓	✓
CR#2	✓	✓	✓	✓
CR#3	✓	✓	✓	✓

Once the positions of the CRs were estimated, the phase at the exact sub-pixel positions were obtained, and converted to slant range change.

CHOICE OF THE REFERENCE POINT

Radar interferometric measurements are relative to each other in space and in time that is, the difference in deformation between points in a certain time interval is observed. In order to reference the measurements to an absolute framework, it is required that the absolute deformation of at least one point, or region, is known, and that this area is observed by the radar measurements.

For this project, CR#1 (Stable Reflector) was designed to be used as reference CRs of the network. Slant range changes of approximately 2.5 mm for CR#2 (Upper Slide Reflector) and 1.7 mm for CR#3 (Lower Slide Reflector) were measured with respect to the reference in 96 days.

SLANT RANGE CHANGE DEFORMATION PROFILE

Table 6 shows the estimated slant range change in millimeters of the CRs. Plots of the time series per reflector and spatial overviews are provided in Figures 6 to 11. Positive slant range change value indicates a target moves away from a satellite.

Table 6. Cumulative slant range deformation in millimeters at the Corner Reflectors. CR#1 was used as reference.

CRs	Sep 25, 2007	Oct 19, 2007	Dec 6, 2007	Dec 30, 2007
CR#1	0.0	0.00	0.00	0.00
CR#2	0.0	-1.10	-2.10	-2.46
CR#3	0.0	0.21	-1.89	-1.66

The standard deviation at the reference reflector (CR#1) was 0.47 mm, which is indicative of the precision of the CRs deformation measurements. The temporal profiles on CR#2 and CR#3 show slant range change of about 2.5 mm and 1.7 mm respectively over three months. The measurements are with respect to the stable reflector CR#1.

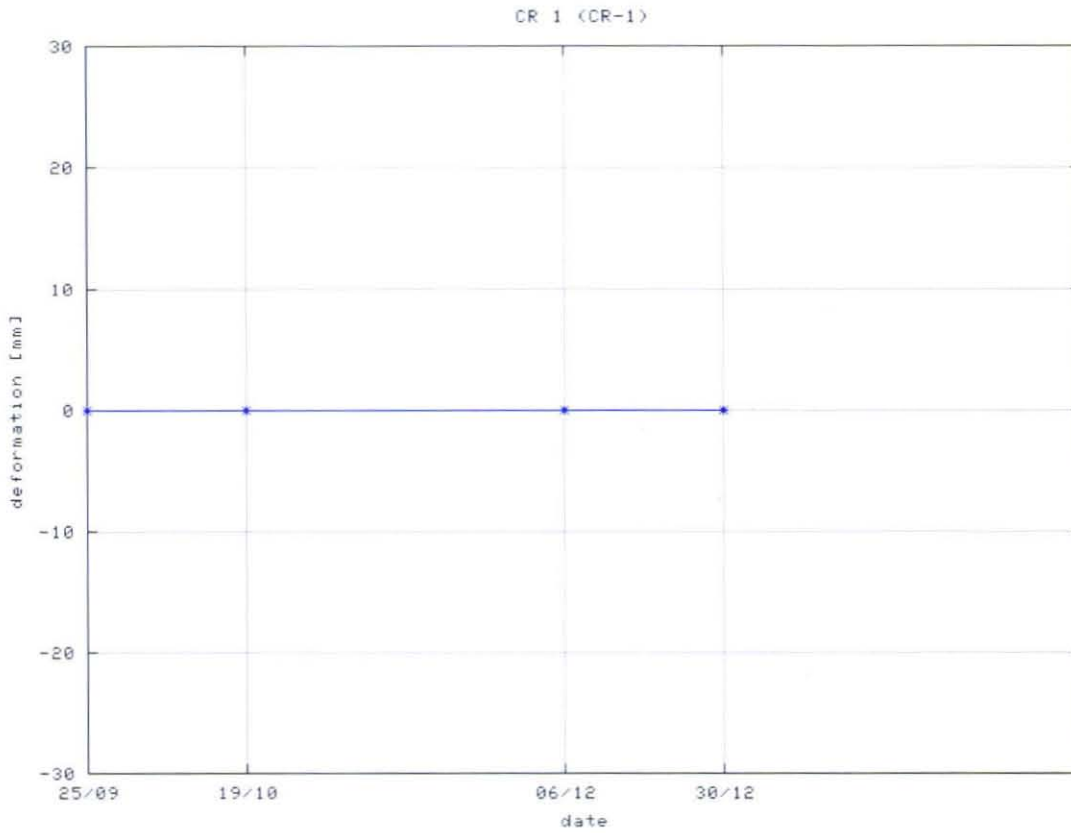


Figure 6. Chart. Slant range change profiles for the installed Corner Reflector #1 (Stable Reflector was used as reference).

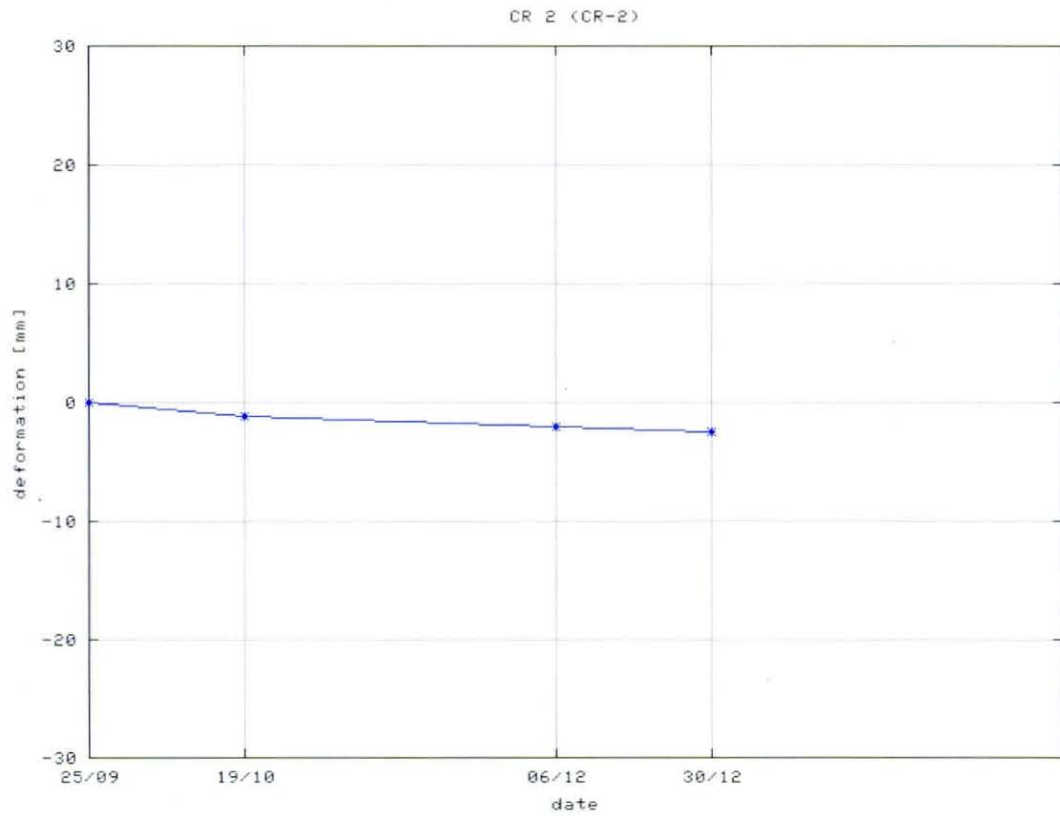


Figure 7. Chart. Slant range change profiles for the installed Corner Reflector #2 (Upper slide reflector).

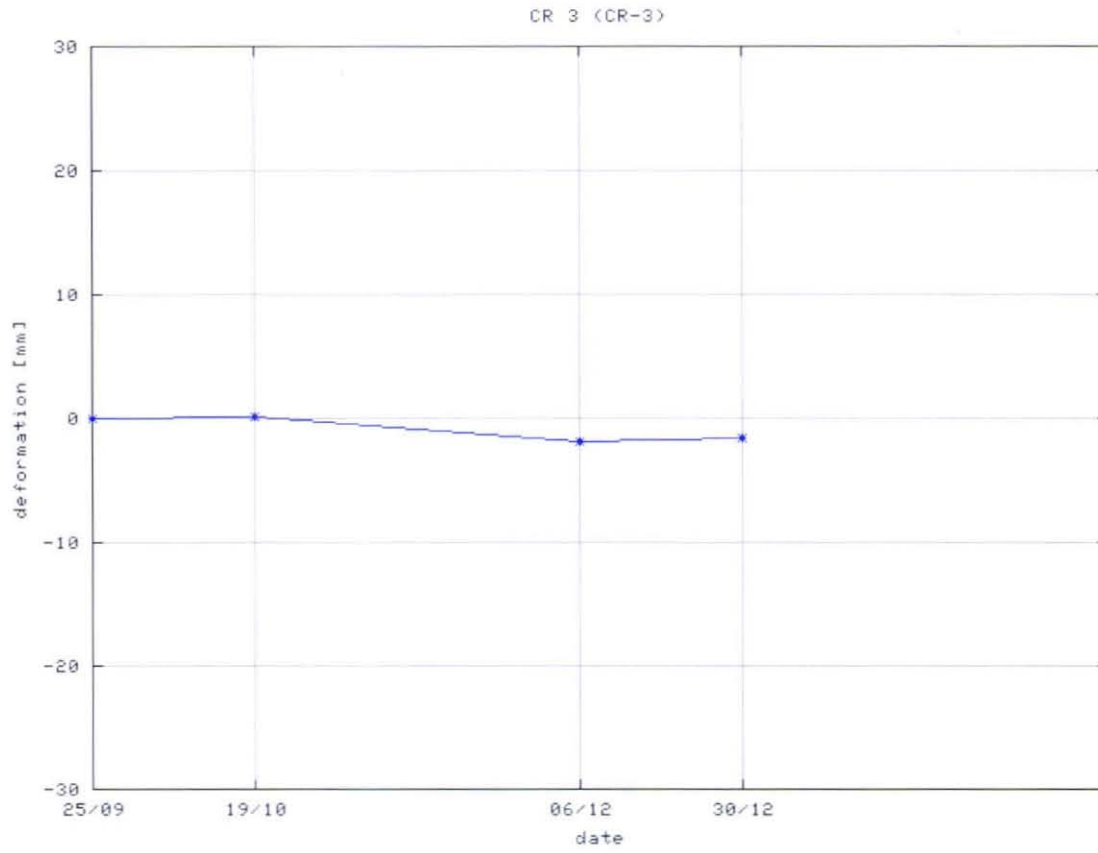


Figure 8. Chart. Slant range change profiles for the installed Corner Reflector #3 (lower slide reflector).

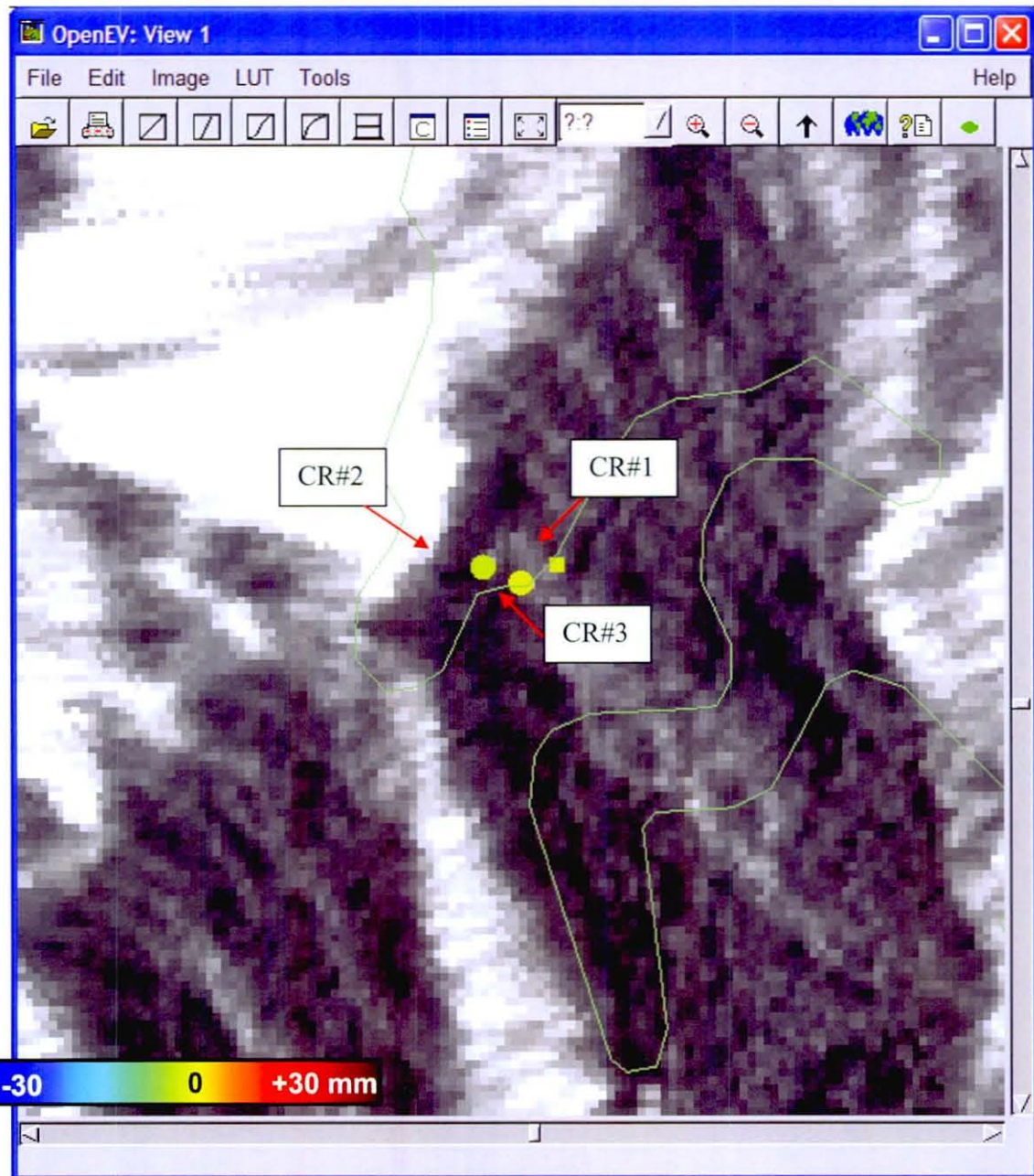


Figure 9. Map. Cumulative slant-range-change from September 25, 2007 to October 19, 2007. The square indicates the reference point (CR#1). The vector data for the General's Highway was approximate.

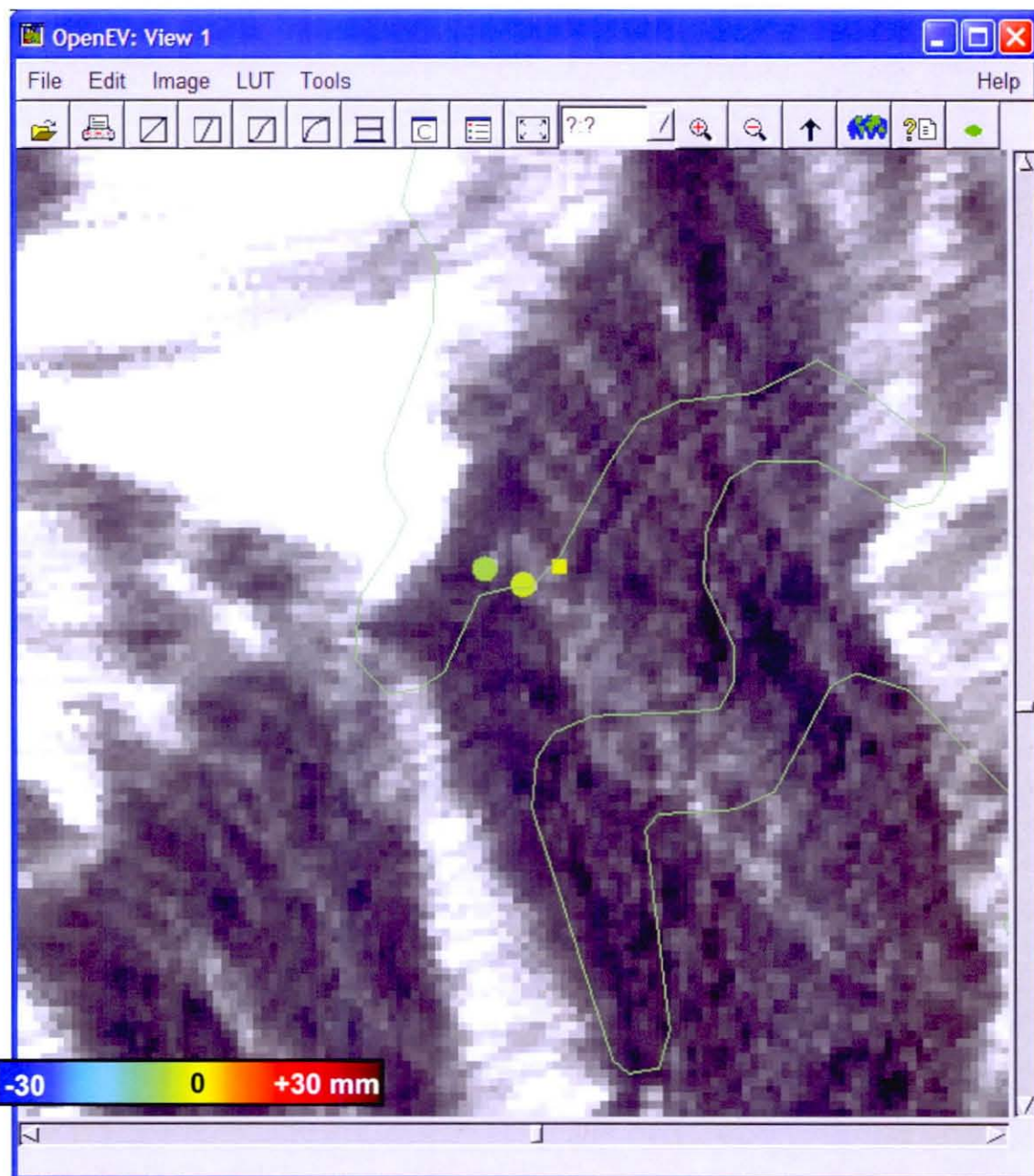


Figure 10. Map. Cumulative slant-range-change from September 25, 2007 to December 6, 2007. The square indicates the reference point (CR#1). The vector data for the General's Highway was approximate.

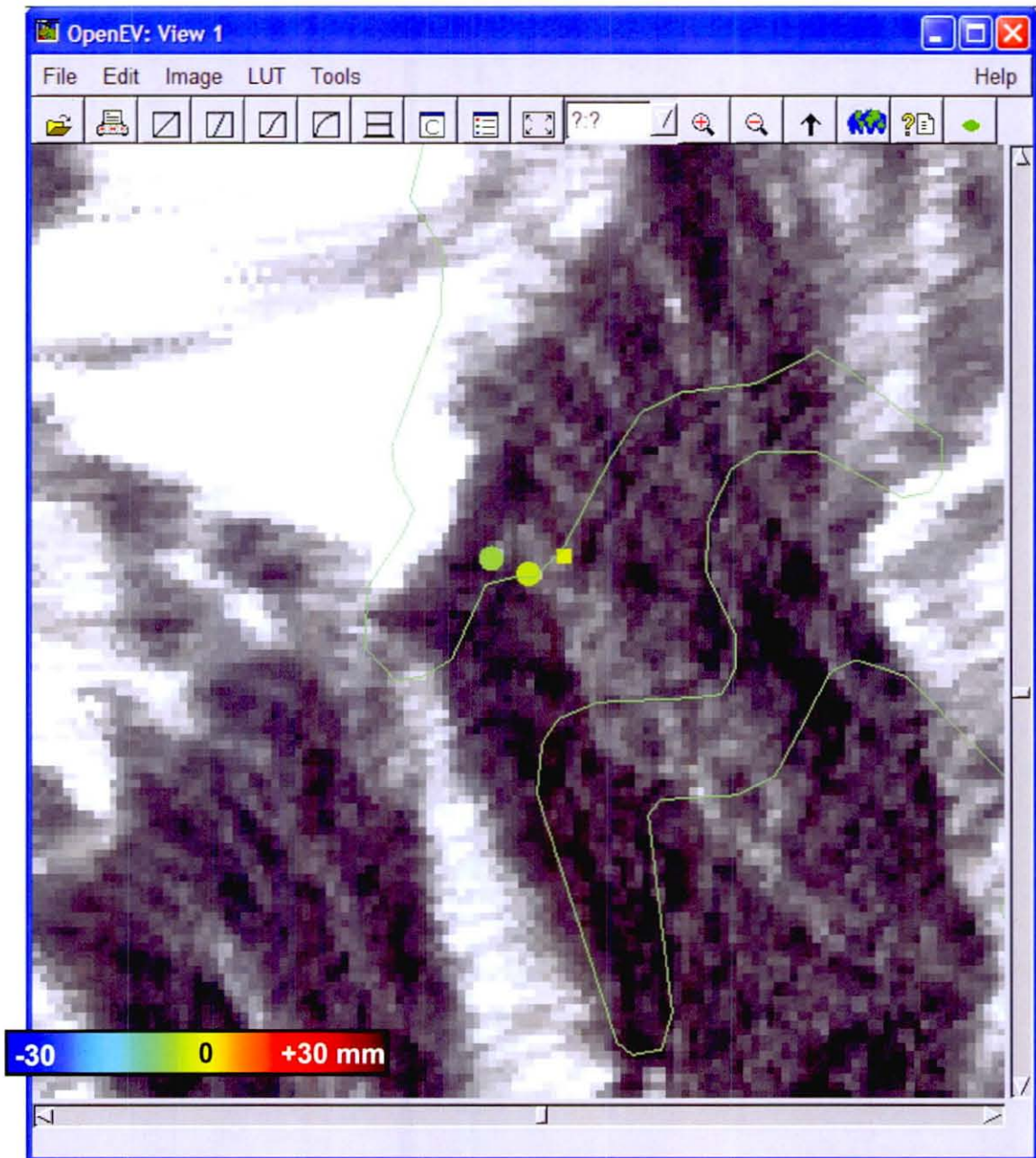


Figure 11. Map. Cumulative slant-range-change from September 25, 2007 to December 30, 2007. The square indicates the reference point (CR#1). The vector data for the General's Highway was approximate.

FLOW-LINE DEFORMATION

Flow-line deformation is slant-range change projected to the steepest direction of the local terrain slope. The local terrain slope consists of a horizontal slope and a vertical slope. The horizontal local terrain slope was obtained by calculating gradient vectors from the input DEM

and the vertical slope for each corner reflector was measured by the CRs installation team. Table 7 lists important parameters used for the flow-line deformation computation. Note that the horizontal slope angle is the angle between the line-of-sight and the actual horizontal slope vector.

Table 7. Parameters used for flow-line deformation computation.

Incidence angle: θ_{inc} [deg]	40.00
Heading [deg]	349.75
Horizontal slope: θ_{hori} [deg]	70.25
Vertical slope: θ_{vert} [deg]	CR #1: 25.0
	CR #2: 50.0
	CR #3: 50.0
Measured slant range: Δr [mm]	CR #1: 0
	CR #2: 2.46
	CR #3: 1.66

Figure 12 shows the geometry for the flow-line deformation computation. The following shows the actual algorithm of the flow-line deformation calculation used for this study.

1. slant range change vector OA (define the vector OA on x-z plane):

$$OA = (\Delta r \cdot \sin \theta_{inc}, 0, \Delta r \cdot \cos \theta_{inc})$$

2. local topographic slope vector OB:

$$OB = (\cos \theta_{hori}, \sin \theta_{hori}, \tan \theta_{vert} \cdot \sin \theta_{hori})$$

3. cosine of the angle BOA:

$$\cos \theta_{BOA} = \frac{OA \cdot OB}{|OA||OB|}$$

4. Flow-line deformation OC:

$$|OC| = \frac{|OA|}{\cos \theta_{BOA}}$$

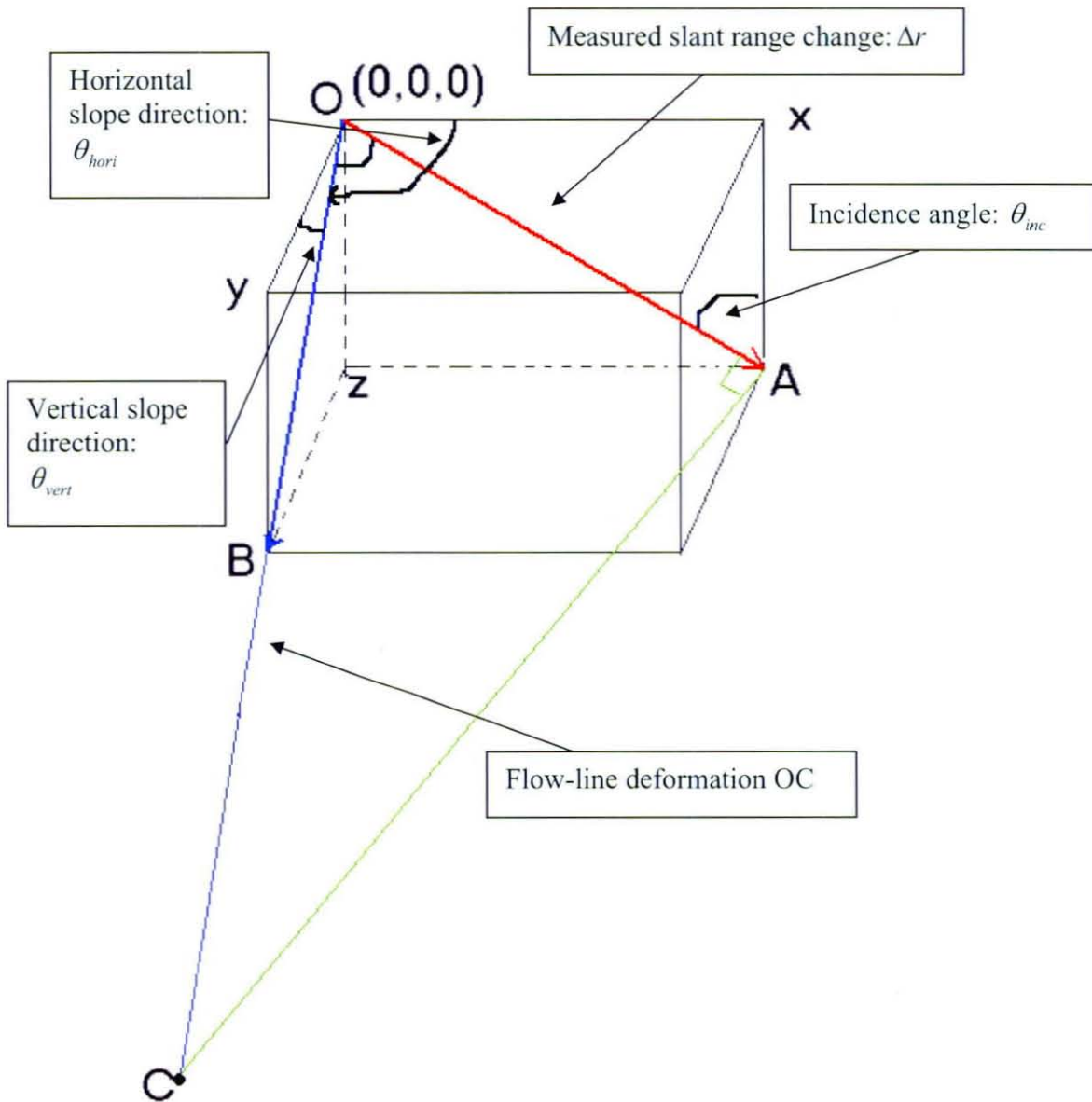
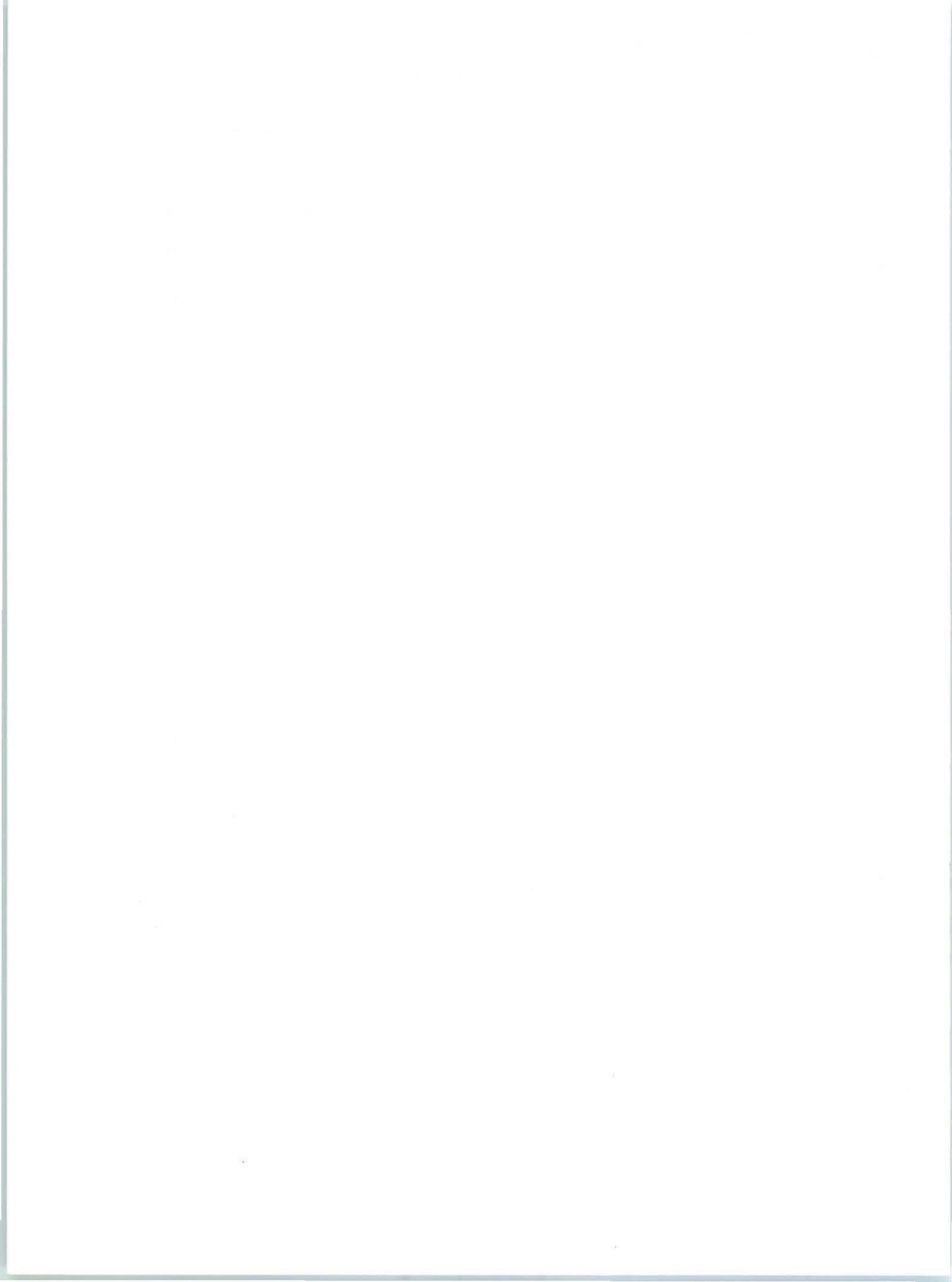


Figure 12. Schematic. Geometry for flow-line deformation computation. An angle between a slant range change vector OA and a local topographic slope vector OB was derived from vector OA and OB . OA and is defined in x - z plane. Note that this is an example only to explain the geometry and it does not depict the actual flow direction.

Table 8 shows the flow-line deformation values converted from the measured slant range change. The direction of the deformation is down-slope. The flow-line deformation is assuming a slant range change is fully caused by deformation on local topographic slope line.

Table 8. Flow-line deformation measurements.

CRS	Absolute measured slant range change (mm)	Flow-line deformation (mm)
CR#1	0.00	0.00
CR#2	2.46	3.43
CR#3	1.66	2.32



CHAPTER 5 – CONVENTIONAL InSAR DEFORMATION MAPS

A deformation map can be generated using conventional InSAR technology if the spatial coherence for an interferometric data pair is above a certain threshold. This product shows the deformation patterns outside of the CRs. In general, for this vegetated area of Sequoia National Park, the noise due to temporal de-correlation (incoherent changes of the positions of the individual scattering elements in a resolution cell, for example, due to vegetation growth) was severe, which prevents conventional interferometry from working, except in certain times of the year in limited areas. That was why the CRs were installed, because they could always be measured at the location of interest. Moreover, the measurements at the CRs provided a better precision.

For conventional interferometric products, the precision of the vertical deformation measurements can be in the order of 3 mm, depending on the level of de-correlation, the perpendicular baseline, and atmospheric circumstances, size of the area of interest, and processing method (it may be possible to measure very precisely between nearby locations if spatial averaging is performed). The conventional interferometric deformation product is particularly useful to detect more severe deformations phenomena, for example, a few centimeters of deformation, or to confirm the absence of such phenomena, as well as to quantify the general shape and extent of deformation areas outside of the CRs locations.

RESULTS

In order to elect the data that contained the most value for this study, all 18 acquired data sets were evaluated as shown earlier in

Table. Pairs were selected that had the largest areas with good quality deformation measurements, and with the best deformation signal-to-noise level. As result, the following deformation maps were generated.

- Pair A for the time period August 8, 2007 to October 19, 2007 (72 days)
- Pair B for the time period December 6, 2007 to December 30, 2007 (24 days)

The noise due to temporal de-correlation was severe for all evaluated interferograms at the location. Figure 13 shows a slant range change map for the time period August 6, 2007, to October 19, 2007. Figure 14 shows a slant range change map for the time period December 6, 2007, to December 30, 2007. No large deformation phenomena were observed in those interferometric data. All deformation maps were calibrated by coherent area surrounding the area of interest. The deformation values on red triangles in Figures 13 and 14 were used for the calibration. Those points were assumed to be stable, and all measurements were relative to those points. Also the layover area and low coherence area (<0.3) were masked out.

For Pair A, the root-mean-square of the observed deformation values in the reference area was ~ 3.5 mm, which was indicative of the precision of the deformation map. For Pair B, the root-mean-square of the observed deformation values in the reference area was ~ 2.6 mm, which also

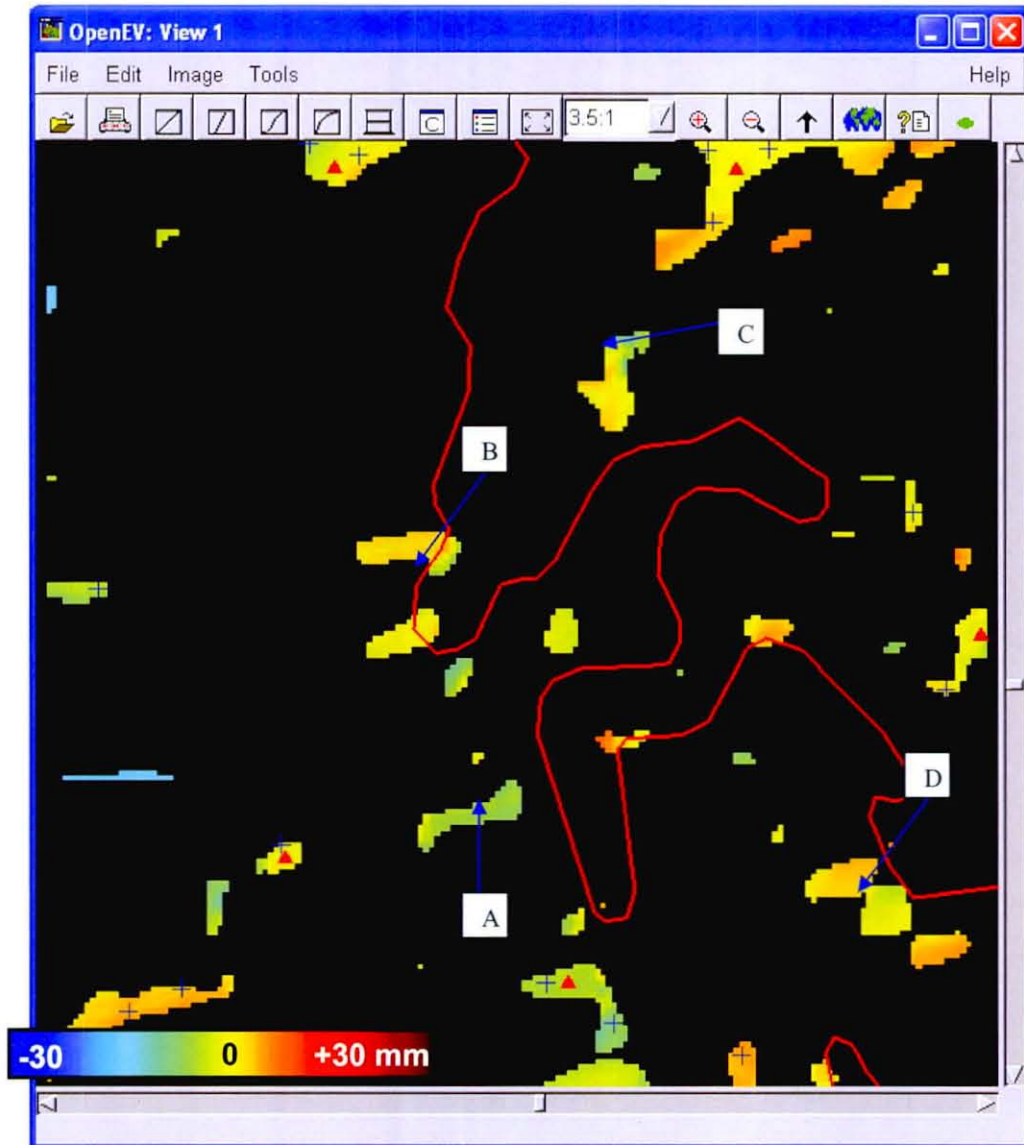


Figure 13. Schematic. Slant range change map for the time period August 8, 2007 to October 19, 2007 (Pair A). The deformation map was calibrated by the deformation values on the red triangles that is, the deformation was relative to this location. Slant range values on blue crosses were used for noise level estimation. Invalid data of low coherence were masked out.

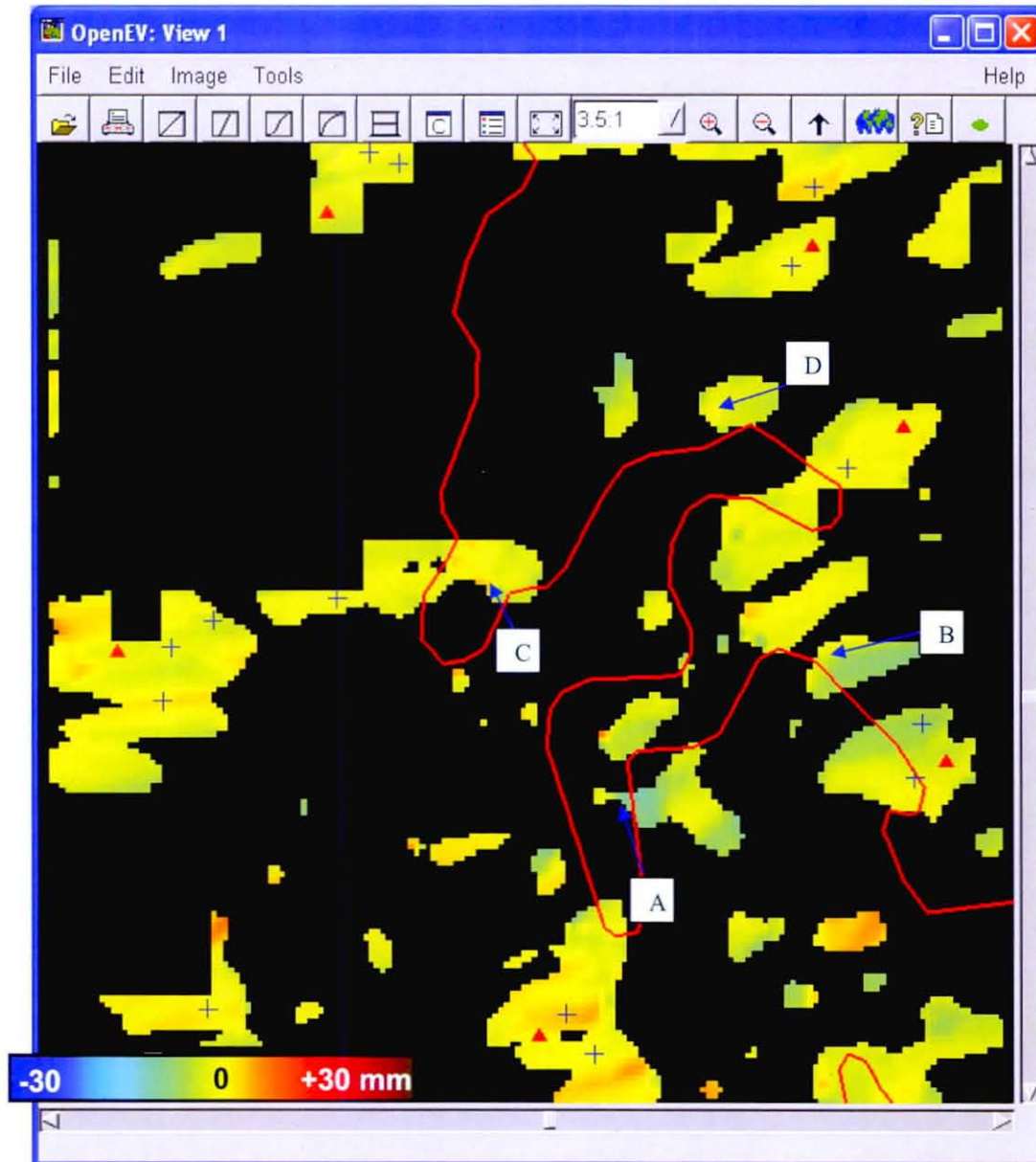


Figure 14. Schematic. Slant range change map for the time period December 6, 2007 to December 30, 2007 (Pair B). The deformation map was calibrated by the deformation values on the red triangles that is, zero deformation was assumed at these locations and the measurements were relative to this reference. Slant range values on blue crosses were used for noise level estimation. Invalid data of low coherence were masked out.

was indicative of the precision of the deformation map. To obtain a 95% confidence interval a factor of 2 was used. Tables 9 and 10 show the deformation measurements for the pairs A and B. Tables 11 and 12 show the estimated noise levels for the Pairs A and B. And, Tables 13 and 14 show the estimated noise level summaries for the Pairs A and B.

Table 9. Deformation measurements from Pair A.

ID	Latitude	Longitude	Deformation (mm)
A	36.5390071	-118.7847545	-4.15
B	36.5427829	-118.7862600	-2.61
C	36.5463759	-118.7826025	-4.76
D	36.5376147	-118.7769527	-2.45

Table 10. Deformation measurements from Pair B.

ID	Latitude	Longitude	Deformation (mm)
A	36.5391785	-118.7819925	-6.44
B	36.5413694	-118.7781349	-5.67
C	36.5426226	-118.7848054	-1.00
D	36.545449	-118.780195	-1.78

Table 11. Estimated noise level of Pair A.

Pixel	Line	Deformation measurements in stable area (m)
120	14	0.00413
130	1	0.00102
47	0	-0.00360
56	2	0.00067
162	98	0.00308
90	151	-0.00336
24	153	0.00459
42	126	-0.00076
9	80	-0.00332
102	158	-0.00598
125	164	0.00552
119	1	0.00020
156	66	0.00109
14	156	0.00482
Noise Level Std Dev (m)		0.00354
95% confidence level		0.00708

Table 12. Estimated noise level of Pair B.

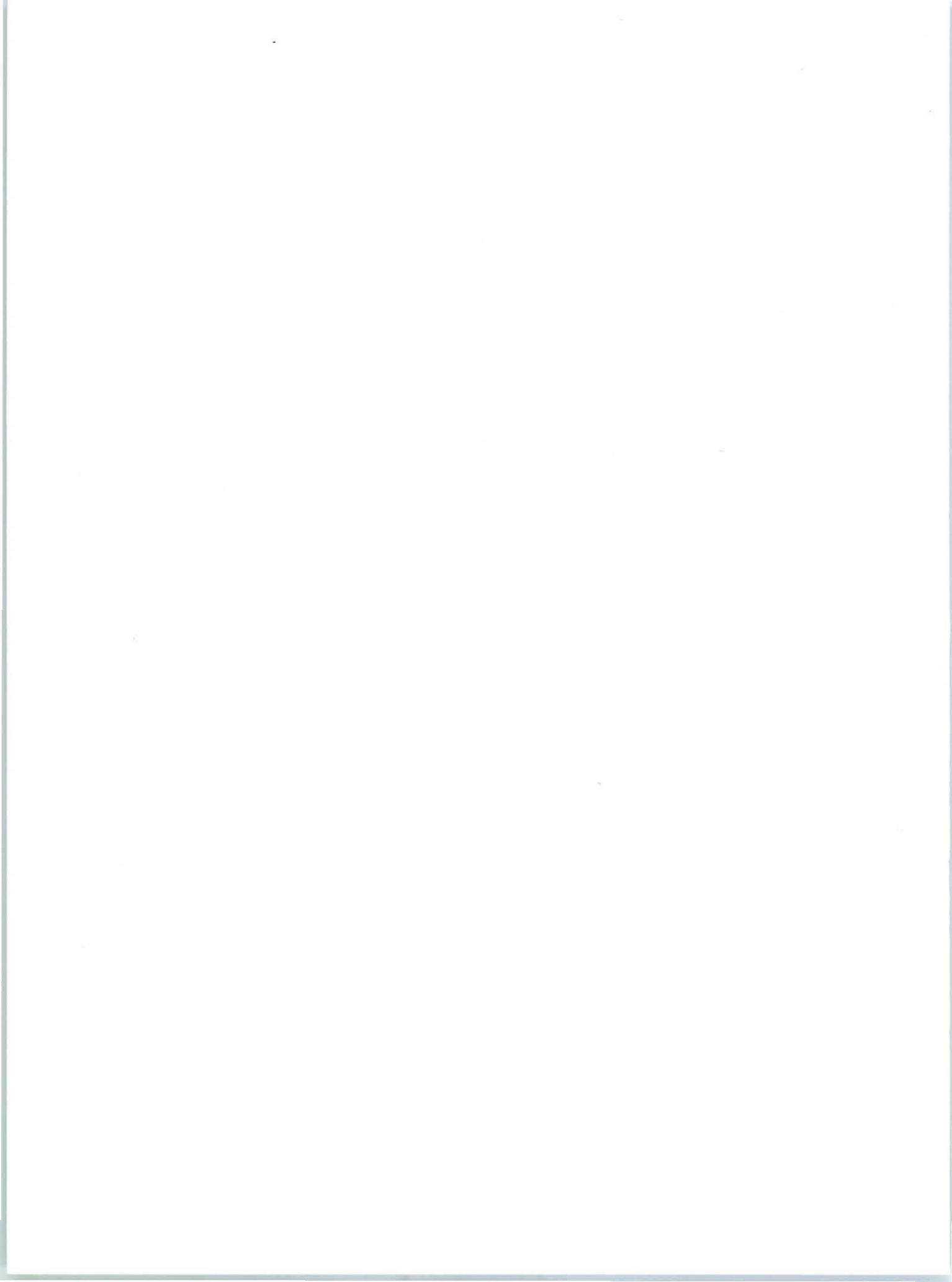
Pixel	Line	Deformation measurements in stable area (m)
22	89	-0.00040
20	98	0.00350
29	84	-0.00165
57	1	0.00166
62	3	-0.00085
132	21	0.00147
136	7	0.00381
142	57	0.00194
154	112	-0.00011
155	102	-0.00509
92	154	0.00492
97	161	0.00115
28	153	0.00245
51	80	0.00087
Noise Level Std Dev (m)		0.00264
95% confidence level		0.00528

Table 13. Estimated noise level summary of Pair A.

Date	Time span	Noise Level standard deviation (mm)	95% Confidence interval (mm)
Aug-8-07 to Oct-19-07	72 days	3.54	7.08

Table 14. Estimated noise level summary of Pair B.

Date	Time span	Noise Level standard deviation (mm)	95% Confidence interval (mm)
Dec-6-07 to Dec-30-07	24 days	2.64	5.28



CHAPTER 6 – CONCLUSIONS

Three CRs were successfully installed on September 17 and 18, 2007, by a team of FHWA in good cooperation with personal of MDA. These CRs were accurately detected and the deformations measured at their locations. Four data sets were available in 2007 after installation of the CRs for measuring the deformation.

Deformation at the CRs was reliably measured. The CRs appeared as bright dots in the radar imagery and were very visible. The noise of the deformation measurements was at the millimeter level, which was apparent from the smoothness of the deformation profile. The measured deformation had a magnitude and direction (down the slope) that appeared very reasonable. The limiting factor in the accurate of the measurements was because of uncertainty of the heights of the installed CRs. The height was not measured during installation and the USGS 10 m DEM was used to obtain the height using bilinear interpolation at the provided position. The deformation measurements were estimated to have a precision of approximately 0.9 mm.

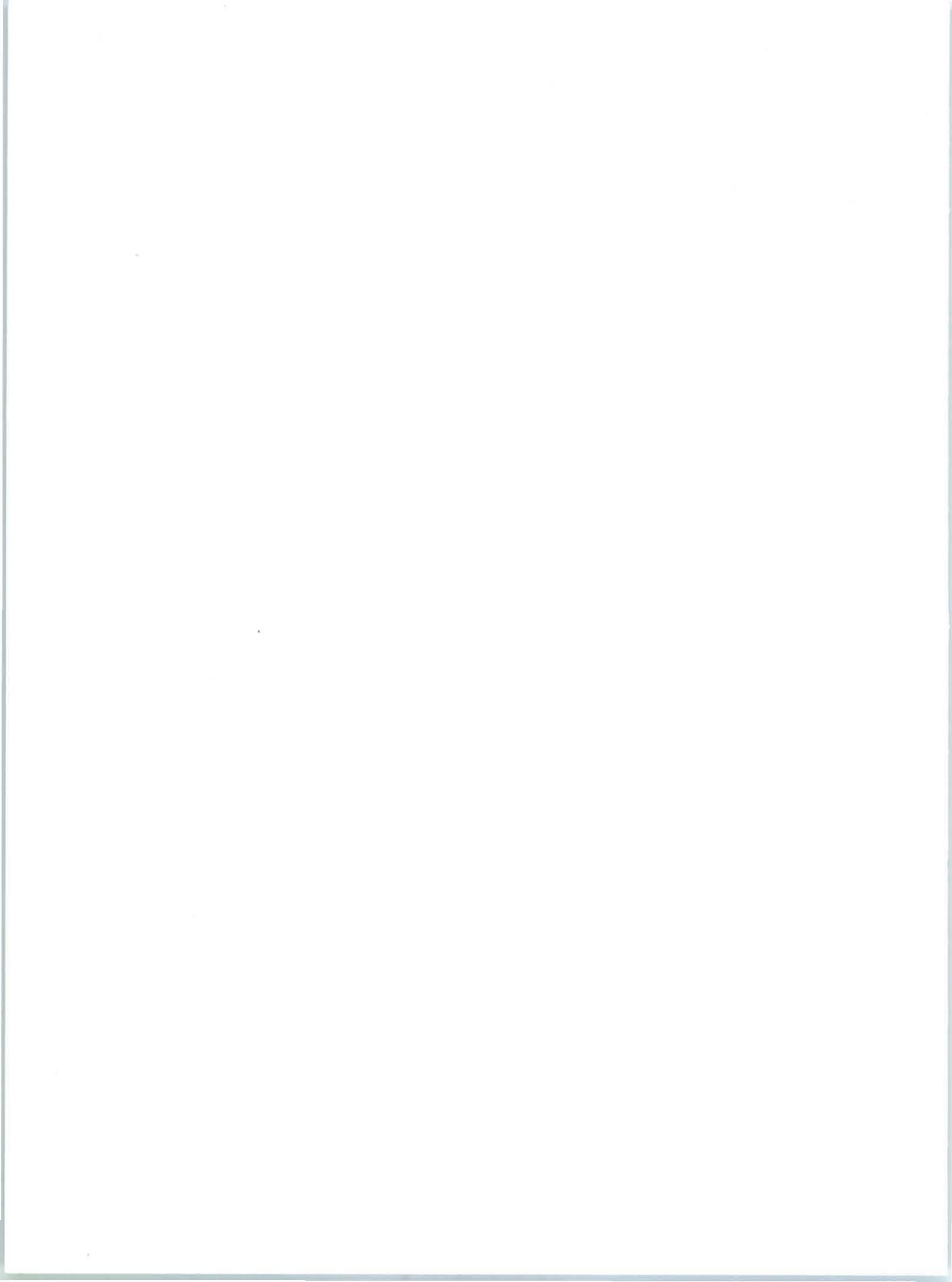
The following observations were made:

- The CRs were well-installed and successful precise deformation measurements were made.
- CR#2 was sliding down in the direction of the local slope by 3.43 mm (flow-line deformation) comparing to CR#1 in the time period from September 25, 2007 to December 30, 2007.
- CR#3 was also sliding down in the direction of the local slope by 2.32 (flow-line deformation) comparing to CR#1 in the time period from September 25, 2007 to December 30, 2007.

Furthermore, two conventional deformation maps were produced for this study. Unfortunately, temporal de-correlation was significant which made it impossible to generate coherent radar interferograms at any time period for this location. Nonetheless, the maps provided some information on the deformation that occurred in the observed time frames.

- Pair A for the time period August 8, 2007 to October 19, 2007 (72 days). ~4 mm of deformation measured in the area with a precision of ~7 mm.
- Pair B for the time period December 6, 2007 to December 30, 2007 (24 days). ~6 mm of deformation measured with a precision of ~5 mm.

The masked out areas due to temporal de-correlation were large. No large deformation phenomena were observed in these deformation maps.

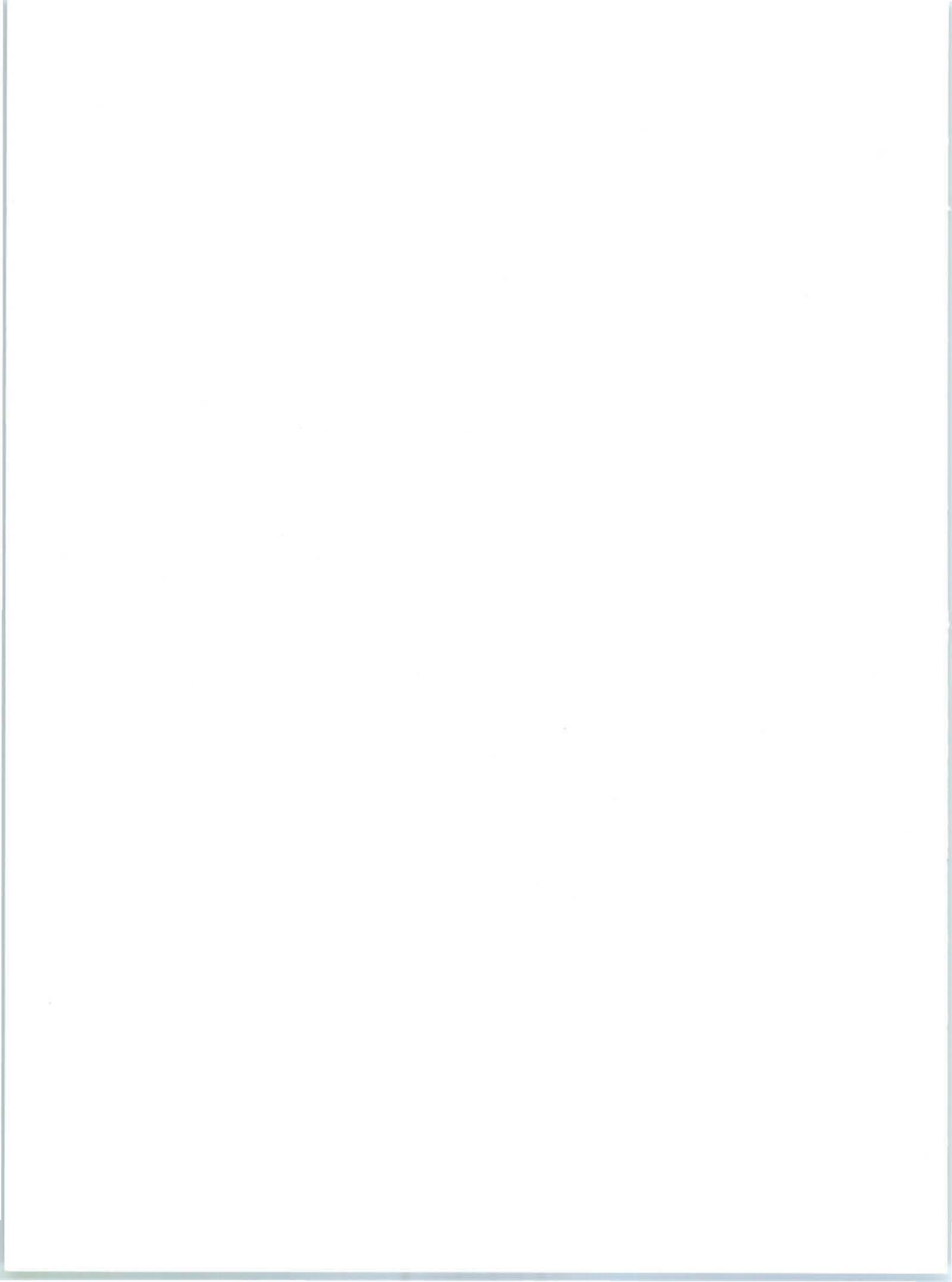


APPENDIX A – EXAMPLE DELIVERABLES

The following information in Table 15 provides examples of the type of files typically delivered for a study like this.

Table 15. Delivered digital files.

Filename	Contents
Generals_Highways_final_report.pdf	This report
Corner Reflectors	
cr_3_4.shp	Shapefile with cumulative deformation from September 25, 2007 to October 19, 2007
cr_3_5.shp	Shapefile with cumulative deformation from September 25, 2007 to December 6, 2007
cr_3_6.shp	Shapefile with cumulative deformation from September 25, 2007 to December 25, 2007
cr_table.xls	Microsoft Excel table with the estimated deformation values and NAD83 positions of the Corner Reflectors
Slant range change maps	
080807_101907_defo.xyz	Slant range change map for the time period August 8, 2007 to October 19, 2007 in ASCII xyz format.
120607_123007_defo.xyz	Slant range change map for the time period December 6, 2007 to December 30, 2007 in ASCII xyz format.



APPENDIX B – NOTES ON CORNER REFLECTOR INSTALLATION

The following is an excerpt of an e-mail report from the FHWA FLH Project Manager shortly after the installation of the Corner Reflectors.

From: Surdahl, Roger
Sent: Thursday, September 27, 2007 1:35 PM
To: Bert KAMPES (and others)
Subject: InSAR Corner Reflector Installation - Sequoia NP

The FHWA Federal Lands Highway and MDA Corporation are cooperating on a project deployment of Interferometric Synthetic Aperture Radar (InSAR) in Sequoia National Park. As part of this effort, we installed three InSAR Corner Reflectors in the Sequoia National Park on September 18 and 19, 2007. The installation was for monitoring of landslide movement on the Generals Highway at about STA 666+00 (English) for the proposed upcoming construction project of CA PRA SEKI 10(8).

On the morning of the first day we assembled the three InSAR units in the Sequoia National Park's maintenance shop. Then we were able to manhandle two of the three into place that each consisted of a 62 lb Corner Reflector head, a 50 lb pipe stand, 3 bags of 50 lb quickcrete, 50 lbs of water, and miscellaneous tools of shovels, crow bar, and trowel for the #1 Stable Reflector and the #3 Lower Slide Reflector.

On the second day however, the access slope and location for the #2 Upper Slide Reflector proved impossible for us to carry the parts of the third unit up the hill manually, so we hired the Park's fire helicopter crew to fly the supplies in for us. All of the Sequoia National Park people were just wonderful and cooperative to work with.

Here is some additional information recorded for each site:

CR#1 Stable Reflector.
N 36 degrees 31.571'¹
W 118 degrees 47.035'
18 degrees to the horizon.
81 feet horizontal (north) offset from roadway centerline.
Mounted on a 25 degree slope.

¹ [MDA] Note that this coordinate is not correct and we assumed it was 32.571'. Moreover, for optimal Corner Reflector processing the 3D position (including the height) is required with an accuracy of ~1m, which was not measured.

CR#2 Upper Slide Reflector.

N 36 degrees 32.568'

W 118 degrees 47.098'

28 degrees to the horizon.

100 feet (estimated) horizontal (north) offset from roadway centerline.

Mounted on a 50 degree slope.

CR#3 Lower Slide Reflector.

N 36 degrees 32.558'

W 118 degrees 47.065'

30 degrees to the horizon.

28 feet horizontal (south) offset from roadway centerline.

Mounted on a 50 degree slope.

We had constructed the mounting plates to position the reflectors 18 degrees up from horizontal. Then once the vertical mounting poles were installed (2 feet deep in 150 lbs of concrete, with 4 feet above ground), we screwed the corner reflectors heads on and pointed them to 253 degrees geographic north. The angle of declination was 13.653 degrees east, so with our compass we actually aligned the reflectors to 139 degrees magnetic north.

Thank you all for your technical, physical, managerial, and financial support for this important study. We look forward to the InSAR results to see how much more effective these reflectors are in further defining the movement on this slide.

Roger W. Surdahl, P.E.
Technology Delivery Engineer
Federal Highway Administration
Central Federal Lands Highway Division
12300 W. Dakota Avenue, Suite 210B
Lakewood, CO 80228

